CrossMark

A Water Cycle Algorithm-Based Multilevel Thresholding System for Color Image Segmentation Using Masi Entropy

Pankaj Kandhway[1] · Ashish Kumar Bhandari[1]

Abstract

In this paper, a recently developed metaheuristic water cycle algorithm (WCA) is coupled with Masi entropy (Masi-WCA) to perform color image segmentation over the optimal threshold value selection process. Masi entropy gives the non-extensive/additive information that exists in an image by a tunable entropic parameter. The water cycle algorithm is a newly established population-based method which has been employed to exploit an optimal value of weighing factors for enforcement of constraints on individual components. The idea behind WCA is grounded on thought of water cycle and how streams and rivers flow downward toward the sea in the real world. The key feature of this paper is to exploit the modern optimization techniques such as water cycle algorithm, monarch butterfly optimization, grasshopper optimization algorithm, bat algorithm, particle swarm optimization, and wind-driven optimization for the color image segmentation purpose. In this paper, two objective (fitness) functions are exploited which are Tsallis and Masi entropy for a fair comparison of the proposed method. The proposed scheme is examined intensively regarding quality, and a statistical graph is included to compare the outcomes of the proposed Masi-WCA method against similar algorithms. Different to other recently developed optimization algorithms used for color image multilevel thresholding operations, WCA presents a better performance in terms of superior quality and fast convergence rate. Experimental evidence encourages the use of WCA for multilevel thresholding with Masi entropy, while it concludes that Tsallis entropy does not outperform over the proposed scheme.

Keywords Multilevel thresholding · Masi entropy · Tsallis entropy · Water cycle algorithm · Grasshopper optimization · Monarch butterfly optimization · Color image segmentation

✉ Ashish Kumar Bhandari
   bhandari.iiitj@gmail.com

Extended author information available on the last page of the article

Ⓑ Birkhäuser

1 Introduction

Color image segmentation is the process of splitting a digital image into distinct non-overlapping homogenous regions according to the similarity in some image features such as color, pattern, intensity value, regional statistics. Segmentation methods are involved as a preprocessing step in various computer vision systems and pattern recognition applications such as edge detection, medical imaging, object detection, video surveillance, classification, industrial production, traffic control system and agriculture fields [1, 5, 12, 15, 22]. Based on the general principle of image segmentation, the taxonomy of different segmentation algorithms can be built which distinguishes the following categories: thresholding methods, edge-based techniques, and region-based techniques. Image segmentation using multilevel thresholding (MT) is one of the leading methods, and thresholding methods play a vital role to accomplish image segmentation. However, most of the techniques are based on the image histogram due to its simplicity, effectiveness, easy to implement, and rapidness. Generally, the thresholding approaches are categorized as bi-level and multilevel thresholding. The easiest one is bi-level thresholding, but for daily-life color images and remote sensing images [9], it does not give optimum results. Among all the remarkable thresholding methods, thresholding based on information entropy theory is a fascinating subject. Entropy-based image segmentation methodology has enticed the devotion of numerous researchers [2, 6, 13, 32, 35] and is considered as one of the prominent global thresholding methods.

Sezgin et al. [42] presented an analysis of image thresholding algorithms and reported that due to the advancements in the information theory, entropy-based thresholding methods have an excessive influence on image segmentation. Pun et al. [34] introduced the concept of entropy-based thresholding for the image segmentation. Afterward, Otsu et al. [3] proposed a method that uses the optimum threshold values by using maximum values of the inter-class variance of gray levels. Kittler and Illingworth have presented a method that optimizes Bayes risk factor to perform thresholding-based segmentation [21]. Kapur et al. [10] proposed a technique that uses the concept of entropy maximization to determine the homogeneousness between classes. A moment preservation principal-based image segmentation approach was developed by Tsai [44] in 1985. In 2015, Bhandari et al. [11] utilized Tsallis entropy, which reports that the information in the image can be treated as either additive or non-additive. A maximum entropy method has been proposed on the basis of non-extensive Tsallis entropy [11] whose entropic parameter q enables the Tsallis entropy to handle the nonadditive information. However, this technique is analogous to maximum entropy method developed by Kapur et al. [10].

In 2006, Sahoo et al. [39] proposed a two-dimensional Tsallis–Havrda–Charvat entropy-based thresholding selection technique. Furthermore, Sahoo [40] has proposed a method for thresholding based on Renyi entropy and this entropy can handle the additive property using the tunable entropic parameter α [20, 37]. The value of α and q can be varied to maximize the Renyi's and Tsallis entropies, respectively. The thresholding approaches have used optimum threshold values by using maximum values of the inter-class variance of gray levels, and based on moment preserving principle [11], cross entropy [23], fuzzy approach [26], and Renyi entropy [39] have also been

successfully used in the segmentation of images. Masi et al. [27] have introduced a new entropic measure, which is based on the analysis of thermodynamic entropies that utilizes the complete probability distribution for image segmentation. Masi entropy has an entropic parameter r, when the value of r is taken to be 1, the Masi entropy [27, 29] reduces to the Shannon entropy [36] which is also known as Boltzmann–Gibbs entropy.

The entropy-based thresholding can be designed as a non-convex multifaceted optimization problem. If the multiple thresholds are treated as the spatial dimensions of the metaheuristics, their parallelism can efficiently address the issue of computational cost of segmented color images by using multilevel color image thresholding-based segmentation. The fitness function of the metaheuristics technique is a standard for choosing the optimum solution. In recent years, entropy is used as a fitness function for the optimization techniques which has drawn the attention of numerous researchers.

In this contexture, several optimization algorithm-based thresholding methods have been developed which use varieties of evolutionary techniques such as artificial bee colony (ABC) motivated from the searching behavior of swarm of honey bees [7, 10], differential evolution [43], genetic algorithm (GA) which is motivated from the notion of survival of the fittest given by Darwin [38], PSO inspired by the public behavior of fish schooling or bird flocking [13, 14], FA which is based on flashing phenomenon of fireflies of tropical areas during summer season [19], WDO other optimization methodology which is grounded on the atmospheric behavior of earth [4, 6], electromagnetism optimization (EMO) which has been inspired by the attraction–repulsion mechanism of the electromagnetism theory [30]. In the recent years, a modified PSO [25]-based multilevel thresholding is applied for the segmentation of medical image segmentation. Recently, a new color image segmentation method has been proposed using entropy thresholding and bat algorithm [28]. The bat algorithm is based on the echolocation of the bats.

In 2017, a new color image multilevel thresholding has been proposed by exploiting backtracking search algorithm (BSA) for satellite images [17]. In favor of color image multilevel thresholding, another new approach has been given [33] through the modification of fuzzy entropy, and further the proposed modified entropic parameters are optimized by Levy flight firefly algorithm to get more accurate results for satellite image segmentation. On the other hand, a new gray-level co-occurrence matrix has been introduced, first time as an objective function to get accurate multilevel thresholding for multiband remote sensing images as well as natural color images [31]. Cuckoo search (CS) [6, 8] and differential evolution (DE) [16] have been reported to solve many multilevel color image segmentation problems for the estimation of optimal threshold values.

Motivated by the successful results in the aforementioned literature, this paper applies different multilevel thresholding approaches for challenging real-life image segmentation problem by using water cycle algorithm (WCA) [18], grasshopper optimization technique (GOA) [41], monarch butterfly optimization (MBO) [46], bat algorithm (BAT) [47], particle swarm optimization (PSO) [24], and wind-driven optimization (WDO) and examines their feasibility for color image thresholding. The WCA, GOA, and MBO are the latest and unexploited optimization techniques for the color image segmentation; these optimization algorithms are inspired by nature. This

paper has been exploited by two objective functions such as Tsallis and Masi entropy criterion for color image segmentation.

Rest of the paper is organized as follows: In Sect. 2, related works are presented through the formulation of Tsallis entropy and different optimization algorithms such as BAT, PSO, WDO, MBO, and GOA. Section 3 presents a detail description of the proposed Masi-WCA-based segmentation approach. Section 4 reports the visual and quantitative results of the proposed technique which are supported by ME, MSE, PSNR, SSIM, FSIM, and entropy. Finally, Sect. 5 concludes the paper by highlighting the main contribution and future scope of the proposed work.

2 Related Works

2.1 Thresholding Criterion for Multilevel Thresholding

Let I denote a test image with an extreme of L gray levels $\{0, 1...L-1\}$ and dimension of the image be $M \times N$. Let $G=\{0, 1...L-1\}$ designates the set of intensity values of the image. The count of pixels with gray level i is denoted by n_i, and the dimension of the image represents a total number of pixels. The pixels of a grayscale or colored image are classified into regions or sets on account of their intensity level (L). This system of arranging the pixels defines the thresholding. For the selection of fitting neighborhoods in a test image, the optimum threshold value (th) should be obtained in a routine, which obeys the simple law of following equations:

$$
\begin{aligned}
C_0 &\leftarrow i \quad \text{if } 0 \leq i \leq \text{th} \\
C_1 &\leftarrow i \quad \text{if th} + 1 \leq i \leq L - 1
\end{aligned}
\tag{1}
$$

where i represents the intensity values of the grayscale image with L, which brings the maximum intensity level. C represents the class of the image.

$$
\begin{aligned}
C_0 &\leftarrow i \quad \text{if } 0 \leq i < \text{th}_1 \\
C_1 &\leftarrow i \quad \text{if th}_1 + 1 \leq i < \text{th}_2 \\
C_2 &\leftarrow i \quad \text{if th}_2 + 1 \leq i < \text{th}_3 \\
C_n &\leftarrow i \quad \text{if th}_n + 1 \leq i < L - 1
\end{aligned}
\tag{2}
$$

where $\{\text{th}_1, \text{th}_2, \text{th}_3,\ldots, \text{th}_n\}$ represents multiple thresholds.

Segmentation of pixels in their respective classes is done using Eqs. (1) and (2) for bi-level and multilevel thresholding, respectively. In the image, the probability of gray level i is estimated by the number of pixels representing the intensity level (frequency of gray level i) occurred in the image, given by Eq. (3):

$$
h_i = \frac{n_i}{M \times N} \quad \text{where,} \quad h_i \geq 0 \text{ and } \sum_{0}^{L-1} h_i = 1.
\tag{3}
$$

The complete probabilistic distribution H of gray levels can be formulated as $H=\{h_0, h1, h2...h_{L-1}\}$. The pixels in the image are separated into two classes (which is bi-level segmentation) as C_0 and C_1 given by Eq. (1), and the pixels in the image are divided into more than two classes (which is multilevel segmentation) as $C_0, C_1,..., C_n$ is given by Eq. (2), Each of the $C_0, C_1, C_2,$ and C_n corresponds to the different object class and background class. Now, the probability of the classes defined for bi-level can be extended for multilevel thresholding, which is formulated by following the equations:

For bi-level thresholding,

$$w_0 = \sum_{i=0}^{\text{th}} h_i, \; w_1 = \sum_{i=\text{th}+1}^{L-1} h_i. \tag{4}$$

For multilevel thresholding,

$$w_0 = \sum_{i=0}^{\text{th}_1} h_i, \; w_1 = \sum_{i=\text{th}_1+1}^{\text{th}_2} h_i, \; w_2 = \sum_{i=\text{th}_2+1}^{\text{th}_3} h_i, \ldots, \; w_n = \sum_{i=\text{th}_n}^{L-1} h_i. \tag{5}$$

The above-defined probability distributions are further normalized. Consequently, a vector of optimal thresholds $\{T_1^*, T_2^*, \ldots, T_n^*\}$ is determined using:

$$\{T_1^*, T_2^*, \ldots, T_n^*\} = \arg\max\{fit(T_1, T_2, \ldots, T_n)\}$$
$$\text{Subject to } 0 \leq T_0 < T_1 < \cdots < T_n \leq L - 1. \tag{6}$$

where fit $(T_1, T_2,...,T_n)$ represents the optimization criterion or objective function, which determines the optimum thresholds for performing multilevel thresholding. Two objective functions used in this paper to compute the optimum threshold values have been discussed in this section.

2.2 Tsallis Thresholding Method

Albuquerque et al. proposed a concept based on Tsallis entropy [11, 39]. The function of thresholding is represented by Eqs. (7) and (8), and the concept of Tsallis entropy has been proposed by Constantino Tsallis. Discrete probabilities make up the notion of Tsallis entropy where the sum of all discrete probabilities is 1. Tsallis entropy is capable of handling nonadditive or non-extensive information [2]. This degree of nonadditivity is represented by the variable q which behaves as an entropic parameter. When the value of q is taken to be 1, the Tsallis entropy reduces to the Shannon entropy which implies that the Tsallis entropy is derived from Shannon entropy. In this paper, the value of q is considered as 0.8 to maximize the Tsallis entropy.

$$E_q(I/\text{th}) = E_q(C_0/\text{th}) + E_q(C_1/\text{th}) + (1-q) \, E_q(C_0/\text{th}) \, E_q(C_1/\text{th}) \tag{7}$$

where

$$E_q(C_0/\text{th}) = \frac{1}{1-q}\left[\sum_{i=0}^{\text{th}}\left(\frac{h_i}{w_o}\right)^q - 1\right]$$

$$E_q(C_1/\text{th}) = \frac{1}{1-q}\left[\sum_{i=\text{th}+1}^{L-1}\left(\frac{h_i}{w_1}\right)^q - 1\right] \tag{8}$$

The maximized Tsallis entropy can be achieved by using Eq. (9) which can be presented as

$$E_T = E_{T_0} + E_{T_1} + E_{T_2} + \cdots + E_{T_n} + (1-q)\, E_{T_n} E_{T_1} E_{T_3} \ldots E_{T_n} \tag{9}$$

where

$$E_{T_0} = \frac{1}{1-q}\left[\sum_{i=0}^{\text{th}_1}\left(\frac{h_i}{w_0}\right)^q - 1\right], \quad w_0 = \sum_{i=0}^{\text{th}_1} h_i$$

$$E_{T_1} = \frac{1}{1-q}\left[\sum_{i=\text{th}_1+1}^{\text{th}_2}\left(\frac{h_i}{w_1}\right)^q - 1\right], \quad w_1 = \sum_{i=\text{th}_1+1}^{\text{th}_2} h_i$$

$$E_{T_2} = \frac{1}{1-q}\left[\sum_{i=\text{th}_2+1}^{\text{th}_3}\left(\frac{h_i}{w_2}\right)^q - 1\right], \quad w_2 = \sum_{i=\text{th}_2+1}^{\text{th}_3} h_i$$

$$E_{T_n} = \frac{1}{1-q}\left[\sum_{i=\text{th}_n+1}^{L-1}\left(\frac{h_i}{w_n}\right)^q - 1\right], \quad w_n = \sum_{i=\text{th}_n+1}^{L-1} h_i \tag{10}$$

where E_{T_i} represents the Tsallis entropy of ith class and the optimal multilevel segmentation problem is solved by assuming n-dimensional problem of optimization. The values of Eq. (10) give the Tsallis entropy of each region (or class), and these values are used in Eq. (9) to get the maximum entropic value. Now, to solve multilevel thresholding problem, n-dimensional optimal thresholds are obtained by Eq. (11), which is used for the maximization of objective function:

$$(T*) = \arg\,\max\left(\sum_{i=0}^{n} E_{T_i}\right) \tag{11}$$

2.3 Bat Algorithm

Xin-She Yang proposed the bat algorithm which is used as a metaheuristic approach for optimization at a global scale. This optimization method is stimulated from the echolocation of micro-bats. The bats use the notion of SONAR echoes to detect their prey and avoid obstacles. The bats transmit the sound waves in the presence of an

object; these waves are reflected back. The time period between the reflection and transmission of the wave impacts the movement of the bats. After the reception of reflected wave, bats use their own pulse to determine the space between them and the prey. The pulse rate ranges from 0 till 1, where 1 represents emission at maximum level and 0 indicates no emission. The loudness of the sound wave and the distance of bat from prey are proportional to each other. In other words, the loudness and pulse rate are inversely proportional to one another [47].

2.4 Particle Swarm Optimization

Particle swarm optimization (PSO) improves the candidate solutions iteratively to get the optimized solution for a problem. It has a population of dubbed particles (or candidate solutions) where these particles are moved in and around in the search space in accordance with few simple formulae which includes the position of the particle and particle's velocity. The movement of each particle is judged by its best-known localized position which is updated when other particles find better positions. This gives high expectation that the swarm is moving toward the optimum solutions. In PSO, search space (possible set of solutions) and possible solution are called as particle position and swarm, respectively. The position representing the best fitness is given as 'P_{best},' and 'G_{best}' defines the best solution of all the particles [24].

2.5 Wind-Driven Optimization

WDO is motivated from the atmosphere of earth, where blowing wind attempts to balance the horizontal air pressure. It is a nature-inspired global optimization method that is created on the ideology of atmospheric motion [4]. It has been shown that wind-driven optimization can be executed easily and is effective in solving the optimization problems. In general terms, WDO has an ability to put in effect the constraints in the search domain. This method is operational on the population-based recursive heuristic global optimization algorithm for multimodal along with multidimensional challenges.

2.6 Monarch Butterfly Optimization

Monarch butterfly optimization (MBO) is a new type of metaheuristic algorithm and inspired from nature; all these butterflies individually are placed in two distinct lands (areas). In the paper [46], the locations of the monarch butterflies are modernized in two techniques. Initially, the offsprings are produced or position-modernized by migration operator and it is adjusted by the migration ratio. This migration behavior of monarch butterflies addresses numerous optimization problems, and it is monitored by some rules. Subsequently, the location of the butterflies is changed by the worth of butterfly adjusting operation [46].

2.7 Grasshopper Optimization Algorithm

Saremi proposed grasshopper optimization algorithm in 2016 which imitates the swarming behavior of grasshoppers. Three components affect the flying route of grasshopper in a swarm. They are a social relationship, gravity, and the horizontal movement of wind. In the GOA algorithm, the most important searching mechanism is a social relationship and the swarming behavior changes significantly when the parameters are changed. The authors have proposed the mathematical model search for grasshopper's interaction and move the swarm closer to the target. In the GOA algorithm, it is estimated that the target is the best solution. While the grasshoppers interact and chase the target, the best solution gets updated if a better solution is found [41].

3 The Proposed Method

In this section, the proposed Masi-WCA approach is demonstrated. Alfred Renyi proposed a definition for the measure of information that preserves expansively for independent events which later termed as Renyi entropy. This entropy quantifies the randomness, uncertainty, or diversity of a system. Renyi entropy is used as a diversity index in statistics and ecology and also essential in quantum information where it is used to measure entanglement [20, 40]. The entropic parameter α defines the amount of extensive information that is present in the image. In a system, the value of α determines which events contribute in the calculation of Renyi entropy. For example, if the value of α tends to 0, almost all the events are weighted equally by Renyi entropy and if a value of α tends to infinity, Renyi entropy is evaluated using the events that have the highest probability. Similarly, in the case of image processing, the events represent the classes of the image whose probabilities are used to determine Renyi entropy. When the value of α is closer to zero, regardless of the probability of each class, Renyi entropy weighs all possible events more equally and when α is one, Renyi entropy reduces to Shannon entropy. This entropy yields maximum result when the value of α is taken to be 0.8.

The property of Tsallis entropy is examined when considering two systems with different temperatures to be in contact with each other and to reach the thermal equilibrium. It is verified that the total Tsallis entropy of the two systems cannot decrease after the contact of the systems. It leads to a generalization of the principle of entropy increase in the framework of non-extensive statistical mechanics. Therefore, a maximum entropy method was proposed based on non-extensive Tsallis entropy [11]. Tsallis entropy is the generalization of Shannon entropy. The pseudo-additivity property of Tsallis entropy with entropic parameter q can handle the non-extensive information for statistically independent subsystems. Sahoo et al. [40] has proposed a method for thresholding based on Renyi entropy. Renyi entropy can handle the additive property using the tunable entropic parameter α [20, 40]. However, Renyi's and Tsallis entropies cannot handle the additive and nonadditive information simultaneously. In the subsequent part, the illustration of the proposed scheme's concept

Birkhäuser

is done using flowchart in Fig. 1. A complete explanation of each step is presented thereafter.

3.1 Masi's Thresholding Method

Masi entropy combines the additivity of Renyi entropy and the non-extensivity of Tsallis entropy. The main argument which deviates Renyi and Tsallis entropies from the Masi entropy is the concordant parameter r. Unlike probability functions of Renyi entropy and Tsallis entropy, where each state probability is raised to the power of their entropic parameters α and q, respectively, in case of Masi, the entire probability function is raised to the power r [27, 29, 36]. The parameter r represents the measure of the degree of extensivity/non-extensivity that might be existent in the system. The entropy-based thresholding methodology is developed on the entropic measure, which is further presented by Masi [27] for gray-level images [29]. Successively, all the entropies directly or indirectly are the generalization of well-established Shannon entropy. The entropic parameter gives the flexibility to achieve different results as the demand entertains. According to the concept of Masi entropy, to obtain an optimal threshold value th, for the bi-level thresholding-based image segmentation is expressed by Eqs. (12) and (13):

$$E_r(I/\text{th}) = E_r(C_0/\text{th}) + E_r(C_1/\text{th}) \tag{12}$$

where

$$E_r(C_0/\text{th}) = \frac{1}{1-r} \log\left[1 - (1-r)\sum_{i=0}^{\text{th}} \left(\frac{h_i}{w_0}\right) \log\left(\frac{h_i}{w_0}\right)\right],$$

$$E_r(C_1/\text{th}) = \frac{1}{1-r} \log\left[1 - (1-r)\sum_{i=\text{th}+1}^{L-1} \left(\frac{h_i}{w_1}\right) \log\left(\frac{h_i}{w_1}\right)\right] \tag{13}$$

The entropy between the two classes C_0 and C_1 is maximized, and the gray level at which this holds true is treated to be the optimal threshold. The complete procedure of the optimal multilevel color image thresholding task is addressed. Basically, entropy is defined as a measurement of randomness, which follows the concept that homogeneous regions will have minimal unpredictability and the non-homogeneous regions will have maximum unpredictability. The higher the value of entropy, the better is the separation between objects and background. The information which exists in pixels of an image has either the additive property or the nonadditive property. In this paper, the value of r is considered as 1.18 to maximize the Masi entropy.

The Masi entropy algorithm is selected for several thresholds that are multilevel thresholding (MT) by maximizing the Masi entropy, and the maximized Masi entropy can be achieved by using Eq. (14) which can be presented as

$$E_{rT} = E_{rT_0} + E_{rT_1} + E_{rT_2} + \cdots + E_{rT_n}, \tag{14}$$

Fig. 1 Flowchart of the
Masi-WCA approach for the
multilevel (thresholding)
segmentation

```
                          ( Start )
                             │
                             ▼
        ┌─────────────────────────────────────────┐
        │   Compute the histogram of the input image │
        └─────────────────────────────────────────┘
                             │
                             ▼
        ┌─────────────────────────────────────────┐
        │         Select the Initial parameters      │
        └─────────────────────────────────────────┘
                             │
                             ▼
        ┌─────────────────────────────────────────┐
        │   Create initial population that is random in │
        │       nature by Eqs. (18), (20), and (21)    │
        └─────────────────────────────────────────┘
                             │
                             ▼
        ┌─────────────────────────────────────────┐
        │  Determine the cost of each raindrop using Eq. (19) │
        └─────────────────────────────────────────┘
                             │
                             ▼
        ┌─────────────────────────────────────────┐
        │   Obtain the intensity of the flow using Eq. (22) │
        └─────────────────────────────────────────┘
                             │
                             ▼
        ┌─────────────────────────────────────────┐
        │   Get the stream flow to rivers by Eq.(24) │
        └─────────────────────────────────────────┘
                             │
                             ▼
        ┌─────────────────────────────────────────┐
        │     Get the rivers flow to sea by Eq.(25)  │
        └─────────────────────────────────────────┘
                             │
                             ▼
        ╱─────────────────────────────────────────╲        No
        │   If the stream has lower function        ├────────┐
        │   (objective function for stream)         │        │
        │   value than corresponding river          │        │
        ╲─────────────────────────────────────────╱         │
                        │ Yes                                 │
                        ▼                                     │
        ┌─────────────────────────────────────────┐          │
        │  Interchange the locations (positions) of │          │
        │    stream with the corresponding river    │          │
        └─────────────────────────────────────────┘          │
                             │◄───────────────────────────────┘
                             ▼
        ╱─────────────────────────────────────────╲        No
        │   If the river has lower function         ├────────┐
        │   (objective function for river)          │        │
        │   value than sea                          │        │
        ╲─────────────────────────────────────────╱         │
                        │ Yes                                 │
                        ▼                                     │
        ┌─────────────────────────────────────────┐          │
        │  Interchange the locations (positions) of │          │
        │         river with the sea                │          │
        └─────────────────────────────────────────┘          │
                             │◄───────────────────────────────┘
                             ▼
        ╱─────────────────────────────────────────╲        No
        │       Evaporation condition fulfilled?    ├────────┐
        ╲─────────────────────────────────────────╱         │
                        │ Yes                                 │
                        ▼                                     │
        ┌─────────────────────────────────────────┐          │
        │   Generate cloud and start raining        │          │
        │   process using Eqs. (27) and (28)        │          │
        └─────────────────────────────────────────┘          │
                             │◄───────────────────────────────┘
                             ▼
        ┌─────────────────────────────────────────┐
        │  Reduce the value of the d_max using Eq. (26) │
        └─────────────────────────────────────────┘
            No               │
        ┌───────────╱─────────────────────────╲
        │           │   Testing the convergence norms │
        │           ╲─────────────────────────╱
        │                    │ Yes
        │                    ▼
        │    ┌─────────────────────────────────────────┐
        │    │   Get the best (optimal) solution and segmented │
        │    │    the input image using optimal solution  │
        │    └─────────────────────────────────────────┘
        │                    │
        │                    ▼
        │                 ( Exit )
```

Reduce the value of the d_{max} using Eq. (26)

where

$$E_{rT_0} = \frac{1}{1-r} \log\left[1 - (1-r) \sum_{i=0}^{\text{th}_1} \left(\frac{h_i}{w_0}\right) \log\left(\frac{h_i}{w_0}\right) \right], \quad w_0 = \sum_{i=0}^{\text{th}_1} h_i$$

$$E_{rT_1} = \frac{1}{1-r} \log\left[1 - (1-r) \sum_{i=\text{th}_1+1}^{\text{th}_2} \left(\frac{h_i}{w_1}\right) \log\left(\frac{h_i}{w_1}\right) \right], \quad w_1 = \sum_{i=\text{th}_1+1}^{\text{th}_2} h_i$$

$$E_{rT_2} = \frac{1}{1-r} \log\left[1 - (1-r) \sum_{i=\text{th}_2+1}^{\text{th}_3} \left(\frac{h_i}{w_2}\right) \log\left(\frac{h_i}{w_2}\right) \right], \quad w_2 = \sum_{i=\text{th}_2+1}^{\text{th}_3} h_i$$

$$E_{rT_n} = \frac{1}{1-r} \log\left[1 - (1-r) \sum_{i=\text{th}_n+1}^{L-1} \left(\frac{h_i}{w_n}\right) \log\left(\frac{h_i}{w_n}\right) \right], \quad w_n = \sum_{i=\text{th}_n+1}^{L-1} h_i \quad (15)$$

where E_{rT_i} represents the Tsallis entropy of ith class and the optimal multilevel segmentation problem is solved by assuming n-dimensional problem of optimization. The values of Eq. (15) give the Masi entropy of each region (or class), and these values are used in Eq. (14) to get the maximum entropic value. Now, to solve multilevel thresholding problem, n-dimensional optimal thresholds are obtained by Eq. (16), which is used for the maximization of objective function:

$$(T*) = \arg \max\left(\sum_{i=0}^{n} E_{rT_i} \right). \quad (16)$$

3.2 Water Cycle Algorithm

Water cycle algorithm (WCA) [18] is a recently proposed metaheuristic technique for optimizing constrained functions and is used for engineering problems. The key objective of WCA is to introduce a new global optimization approach for finding the constrained optimization complications. Hence, a new population-based algorithm is proposed named as the water cycle algorithm (WCA) method and the idea behind the WCA is grounded on a thought of water cycle and how streams and rivers flow downward toward the sea in the real world. WCA is motivated by nature, and it includes four important sub-parts, e.g., create the initial population, a stream flow to the rivers or sea, evaporation condition, and raining process.

3.2.1 Create the Initial Population

For solving an optimization problem via population-based metaheuristic techniques, the values of problem variables are designed as an array. This array is known as 'Raindrop' for a single solution. For a M_{var} dimensional optimization problem, the

values are represented as an array for a raindrop of $1 \times M_{\text{var}}$. This array is expressed in Eq. (17).

$$\text{Raindrop} = [y_1, y_2, y_3, \ldots, y_M]. \tag{17}$$

For the optimization approach, a matrix of raindrops of size $M_{\text{pop}} \times M_{\text{var}}$ is created that is represented as the population of raindrops. Therefore, the matrix Y is produced randomly, where rows and column are given as the population size (M_{pop}) and the design variable size (M_{var}), respectively.

$$\text{Population of raindrops} = \begin{bmatrix} \text{raindrop}_1 \\ \text{raindrop}_2 \\ \vdots \\ \text{raindrop}_{M_{\text{pop}}} \end{bmatrix} = \begin{bmatrix} y_1^1 & y_2^1 & \cdots & y_{M_{\text{var}}}^1 \\ y_1^2 & y_2^2 & \cdots & y_{M_{\text{var}}}^2 \\ \vdots & \vdots & \vdots & \vdots \\ y_1^{M_{\text{pop}}} & y_2^{M_{\text{pop}}} & \cdots & y_{M_{\text{var}}}^{M_{\text{pop}}} \end{bmatrix}. \tag{18}$$

The values of each decision variable ($y_1, y_2, \ldots, y_{M_{\text{var}}}$) are signified as floating point number, that is, real values or a predefined set for discrete and continuous problems, respectively. A raindrop cost is achieved by the calculation of cost function (C) expressed in Eq. (19).

$$C_j = \text{Cost}_j = f\left(x_1^j, x_2^j, \ldots, x_{N_{\text{var}}}^j\right) \quad j = 1, 2, 3, \ldots, M_{\text{pop}}. \tag{19}$$

The best individuals are chosen from rivers and sea that gives a number of M_{sr}, and the raindrops contained minimum value among others that is considered as a sea, where M_{sr} is the summation of user parameter, that is, the number of rivers and a single sea. The remaining population, that is, raindrops from the streams which flow to the rivers or may directly flow to the sea, is obtained and represented in Eq. (21).

$$M_{\text{sr}} = \text{Number of Rivers} + \underbrace{1}_{\text{Sea}} \tag{20}$$

$$M_{\text{Raindrops}} = M_{\text{pop}} - M_{\text{sr}}. \tag{21}$$

The assigned raindrops to the sea and rivers depend on the flow intensity and are expressed in Eq. (22).

$$\text{NS}_n = \text{round}\left\{ \left| \frac{\text{Cost}_m}{\sum_{j=1}^{M_{\text{sr}}} \text{Cost}_j} \right| \times M_{\text{Raindrops}} \right\}, \quad m = 1, 2, \ldots, M_{\text{sr}}, \tag{22}$$

where NS_n represents the number of streams which flow to the specific rivers or sea.

3.2.2 A Stream Flow to the Rivers or Sea

The streams are formed by the raindrops, and these streams are connected to each other to form new rivers. Some of the streams may also flow directly to the sea, and

all streams and rivers finish in a sea that gives best optimal solution (point). The connecting line of a stream flows to river and uses randomly chosen distance, which is defined as follows in Eq. (23).

$$Y \in (0, C \times d), \quad C > 1, \tag{23}$$

where d is represented as the current distance between stream and river. The value of Y in Eq. (23) corresponds to a distributed random number between 0 and ($C \times d$). A value of C is between 1 and 2; for the best solution, it should be 2 or near to 2. The C value greater than 1 enables streams to flow in altered directions toward the rivers. Hence, the new position for rivers and streams is defined as:

$$Y_{\text{Stream}}^{j+1} = Y_{\text{Stream}}^{j} + \text{rand} \times C \times \left(Y_{\text{River}}^{j} - Y_{\text{Stream}}^{j} \right) \tag{24}$$

$$Y_{\text{River}}^{j+1} = Y_{\text{River}}^{j} + \text{rand} \times C \times \left(Y_{\text{Sea}}^{j} - Y_{\text{River}}^{j} \right), \tag{25}$$

where the value of the function rand is a generated random number between 0 and 1 that is uniformly distributed. The solution of the stream is better than its connecting river, the locations of stream and river are swapped, and this criterion is also applied for rivers and sea.

3.2.3 Evaporation Condition

The most important factor of the WCA is evaporation that prevents the method from rapid convergence or the immature convergence. The evaporated (vaporized) water is carried into the atmosphere to produce clouds and then condenses in the colder atmosphere, liberating the water back to earth in the form of rain. This rain generates the new streams and follows the conditions which have been mentioned above. The complete process or cycle is called water cycle. The pseudocode gives an idea about how to define whether or not river flows to the sea.

$$\text{if } \left| Y_{\text{Sea}}^{j} - Y_{\text{River}}^{j} \right| < d_{\max}$$
$$j = 1,2,3,\ldots,\text{M}_{\text{sr}} - 1$$
$$\text{Evaporation and raining process}$$
$$\text{end}$$

where the value of $d_{\max}$ is close to zero (small number). The distance between sea and a river is less than $d_{\max}$. This condition specifies that the river has linked the sea, and the evaporation and raining process are applied. Otherwise, it reduces the search and a small value inspires the search intensity near the sea. The value of $d_{\max}$ adaptively decreases as:

$$d_{\max}^{j+1} = d_{\max}^{j} - \frac{d_{\max}^{j}}{\text{max iteration}}. \tag{26}$$

3.2.4 Raining Process

In this part, the new raindrops formed streams in the different positions or location. The new positions of the recently formed streams can be found exactly and clearly with the help of the following equation.

$$Y_{\text{Stream}}^{\text{new}} = \text{LB} + \text{rand} \times (\text{UB} - \text{LB}), \qquad (27)$$

where LB and UB are represented as lower and upper bounds, respectively. Equation (29) is described only for streams which directly flow to the sea, and the core idea of this equation is to inspire the generation of the stream to improve the exploration near the sea in the possible state for difficulties.

$$Y_{\text{stream}}^{\text{new}} = Y_{\text{sea}} + \sqrt{\mu} \times \text{rand}n(1, M_{\text{var}}), \qquad (28)$$

where μ represents a coefficient which gives the range of searching states (region) near the sea, rand$n$ defines a random number which is normally distributed, and the value for μ is set to 0.1. From this equation, the created individuals with variance μ are distributed around the best-obtained optimum point.

The detailed steps of the proposed Masi-based color image multilevel thresholding operation are described, and the flowchart of the pseudocode of Masi-WCA method is shown in Fig. 1.

Step 1 An input image I is taken, if I is a color image then it is separated into three bands (Red–Green–Blue) and grayscale image is directly used.

Step 2 Compute the histogram of each band of the color image.

Step 3 Allocate the control parameters of WCA such as population size (M_{pop}), number of design variable (M_{var}), number of iterations (stopping criterion), objective function, threshold levels.

Step 4 Generate the optimum thresholds by maximizing an objective function (or minimizing the negative of the entropy value) following the below pseudocode of WCA:

> *Pseudo code of WCA algorithm*
> - *Assign input parameters for WCA that are $M_{pop}, M_{var}, M_{sr}, d_{max}$, and max iteration.*
> - *Find the number of streams for rivers and sea using Eqs. (20) and (21).*
> - *Generate initial population that is random in nature.*
> - *Describe the intensity of flow with help of Eq. (22)*
>   *while $(tr < max\ iteration)$ or $(any\ stopping\ condition\ )$*
>   *for $j = 1$: population size $\left(M_{pop}\right)$*
>   *Using Eqs. (24) and (25) for the stream flows to its corresponding rivers and sea*
>   *if $F\_New\_Stream < F\_River$*
>   *River $=$ New$\_$Stream;*
>   *if $F\_New\_stream < F\_Sea$*
>   *Sea $=$ New$\_$Stream;*
>   *end if*
>   *end if*
>   *Estimate the objective function*
>   *end for*
>   *for $j = 1 : M_{sr}$*
>   *if $(distance\ (\ River\ and\ Sea\ ) < d_{max}) or\ (rand\ < 0.1)$*
>   *New streams are generated using Eq. (27)*
>   *end if*
>   *end for*
>   *Decrease the d_{max} using Eq. (26)*
>   *end while*
>   *Postprocess results and visualization*

Step 5 The search intensity near the sea (the optimum solution) is used. The current best solution (optimum solution) for each of the color channels represents the set of optimal threshold values (T_R, T_G, and T_B,) with best maximum objective function value.

Step 6 Each color channel is segmented individually using the corresponding threshold values. The segmented color channels are then concatenated to form the segmented color image.

4 Experimental Results and Discussion

In this section, experiment results have been discussed to evaluate the performance of the proposed Masi-WCA method over other methods for multilevel thresholding of the color images. The segmented results have been evaluated over 10 daily-life color images, and each color image is a multidimensional image with multimodal nature due to the presence of different bands (RGB). Input images and histogram plots of each band are shown in Fig. 2. Moreover, the presence of dense and complex features requires a sophisticated and accurate multilevel thresholding algorithm for the detection and identification of the region of interest. Each of the test images is segmented into four different thresholding levels: 3-level, 5-level, 8-level, and 12-level thresholding to achieve segmentation. All the algorithms are implemented using MATLAB R2017a on a personal computer with 3.4 GHz Intel Core-i7 CPU, 8 GB RAM running on Windows 10 system. Each of the test images is independently run 50 times using
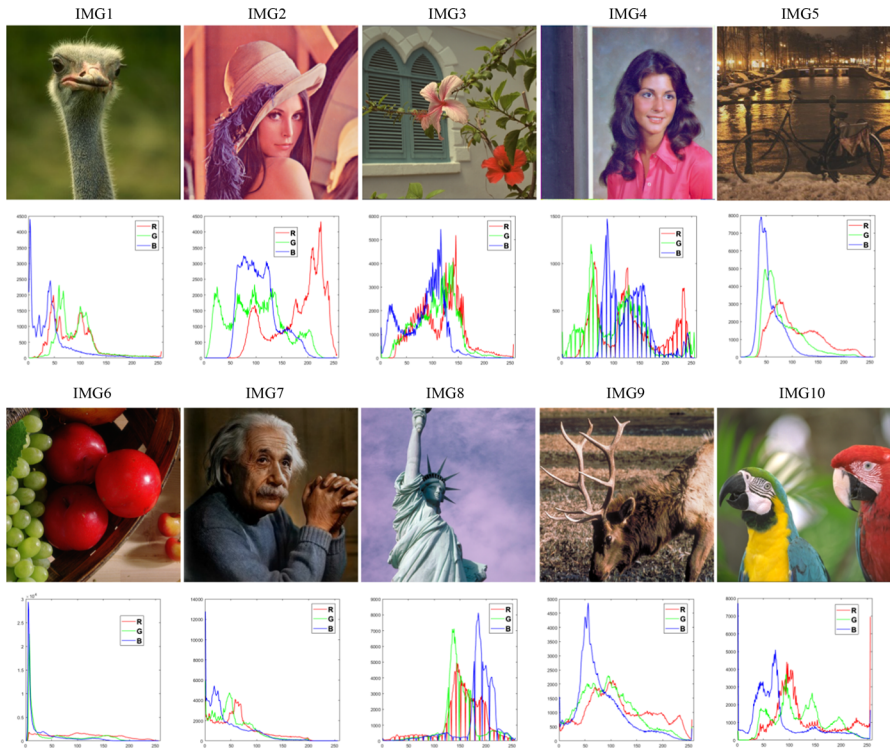
Fig. 2 Test color images (IMG1, IMG2, IMG3, IMG4, IMG5, IMG6, IMG7 IMG8, IMG9, and IMG10) and corresponding histogram plot of each frame (R–G–B) of the color images (Color figure online)

all algorithms to avoid any stochastic discrepancy due to the random nature of the optimization algorithm. For all the optimization algorithms, the population size and the number of iterations are set as 15 and 200 to provide fairness and convenience for performance comparison between WCA and other compared optimization algorithms.

4.1 Image Quality Measures

The objective function value depends on the mathematical modeling of the objective function and the architecture and search strategy of the optimization algorithms. The objective function value indicates toward the best or worst segmentation quality of the algorithm. The computation time of an algorithm depends on the complexity of the method. The complexity of the method depends upon the mathematical structure of its objective function and the structure of the optimization algorithm. Therefore, to test the efficiency of any algorithm, computation time is an important parameter to be computed. The time taken by any technique to perform the segmented output is directly proportional to the complexity of that algorithm. The computation time also increases as the number of thresholding level increases.

Table 1 Fidelity parameters considered to test the efficiency of the proposed method with other algorithms

S. No.	Parameters	Formula	Remarks
1.	Misclassification error (ME) [29]	$\text{ME} = 1 - \dfrac{|B_O \cap B_T| + |F_O \cap F_T|}{|B_O| + |F_O|}$	ME relates to the wrong assignment of foreground pixels to the background or background pixels to the foreground
2.	Mean square error (MSE) [10]	$\text{MSE} = \dfrac{\sum_{i=1}^{M} \sum_{j=1}^{N} \left(I(i,j) - I'(i,j)\right)^2}{MN}$	Calculates the difference between expected value and the actual value
3.	Peak signal-to-noise ratio (PSNR) [11]	$\text{PSNR(in dB)} = 20 \log_{10}\left(255/\sqrt{\text{MSE}}\right)$	It is the ratio of maximum power of a signal to the power of noise
4.	Structural similarity index (SSIM) [45]	$\text{SSIM}(I, I') = \dfrac{(2\mu_I \mu_{I'} + l_1)(2\sigma_{II'} + l_2)}{(\mu_I^2 + \mu_{I'}^2 + l_1)(\sigma_I^2 + \sigma_{I'}^2 + l_2)}$	Evaluates the similarity between the segmented image and the original image
5.	Feature similarity index (FSIM) [48]	$\text{FSIM} = \dfrac{\sum_{c=1}^{N} S_D(c)\text{PCmax}(c)}{\sum_{c=1}^{N} \text{PCmax}(c)}$	Calculates the feature similarity of segmented image and the original image
6.	Entropy [29]	$\text{Entropy} = \sum_i P_i \log_2 P_i$	Indicates the average information of an image

To provide a comprehensive performance assessment of each algorithm, different fidelity parameters such as best objective function values, computation time (in seconds), misclassification error (ME), peak signal-to-noise ratio (PSNR), mean square error (MSE), feature similarity index (FSIM), structural similarity index (SSIM), and entropy are included in Table 1. A comprehensive discussion of the experimental results has been presented in this section. Therefore, the computed segmented results for each test image using Tsallis and Masi entropies as fitness function have been evaluated using BAT, PSO, WDO, MBO, GOA, and WCA. Keeping the view of Tables 2, 3, 4, 5, 6, 7, 8, and 9, Masi-WCA has outperformed in comparison with other optimization techniques (BAT, PSO, WDO, MBO, and GOA) as well as Tsallis entropy-based fitness function.

4.2 Experiment 1: Tsallis Entropy

The results achieved for each test image by using Tsallis entropy as an objective (or fitness) function are discussed and evaluated in this section. In the case of Tsallis entropy, it is easy to confirm which optimization technique has produced superior performance due to an optimal value of ME, MSE, PSNR, SSIM, FSIM, and entropy for the maximum number of cases. The metaheuristic methods are stochastic in behaviors

Table 2 Comparison of best objective values (entropy) and ME computed by different algorithms using Tsalli entropy

Test Images	m	Best objective values						ME					
		BAT	PSO	WDO	MBO	GOA	WCA	BAT	PSO	WDO	MBO	GOA	WCA
IMG1	3	23.6625	24.0533	23.9536	23.6781	24.0617	24.0600	0.3524	0.4162	0.5643	0.4184	0.4184	0.4184
	5	30.8518	31.0922	31.1790	30.8247	31.2057	31.1844	0.2458	0.2313	0.3681	0.1495	0.2607	0.1595
	8	38.5848	39.7181	39.0562	38.1332	39.7252	39.9561	0.1024	0.1436	0.1555	0.1630	0.0952	0.0932
	12	47.4674	48.4684	49.2492	47.3112	49.4166	49.8127	0.0854	0.0683	0.1506	0.1355	0.0828	0.0827
IMG2	3	22.4017	22.6702	22.6698	22.5428	22.6706	22.6705	0.2954	0.2771	0.2731	0.2229	0.2749	0.2733
	5	28.8023	29.0605	29.1217	28.6063	29.1560	29.1555	0.1547	0.1499	0.1913	0.1410	0.1508	0.1508
	8	35.4117	36.6402	37.2726	36.0717	37.3011	37.1190	0.1245	0.0857	0.1045	0.0657	0.1025	0.0549
	12	42.8853	45.0334	45.6237	43.0182	45.6693	45.8490	0.0824	0.0309	0.0190	0.0153	0.0110	0.0090
IMG3	3	23.5911	23.9655	23.9135	23.6810	23.9882	23.8882	0.2845	0.3254	0.3061	0.2515	0.2175	0.2175
	5	30.3331	31.1887	31.3589	31.0935	31.3577	31.3164	0.1859	0.1750	0.1496	0.1439	0.1610	0.1368
	8	38.0343	39.7592	40.3236	39.4158	40.3273	40.2197	0.0842	0.0984	0.1063	0.0904	0.0917	0.0710
	12	47.4535	48.6091	49.4703	47.4568	49.5093	49.2301	0.0524	0.0332	0.0954	0.0597	0.0604	0.0332
IMG4	3	21.9057	22.0597	22.0894	21.8900	22.9145	22.0783	0.3148	0.3103	0.2986	0.2712	0.4393	0.3340
	5	27.9494	28.5781	28.5787	28.4820	28.6246	28.5626	0.2497	0.1875	0.2657	0.1612	0.3413	0.0609
	8	35.0129	36.4026	36.8213	35.7984	36.8392	37.0327	0.1145	0.0879	0.1336	0.0602	0.0455	0.0401
	12	43.2593	44.1975	45.2234	42.3860	45.7143	45.3410	0.0345	0.0060	0.0193	0.0213	0.0361	0.0162
IMG5	3	23.1362	23.3392	23.3464	23.1079	23.3465	23.3459	0.6248	0.6221	0.6278	0.6603	0.6231	0.6201
	5	28.7548	30.2588	30.2993	29.8523	30.2997	30.2850	0.4912	0.4819	0.4818	0.4549	0.4711	0.4438
	8	36.3362	38.1366	38.7655	37.9012	38.8626	38.5558	0.3586	0.3438	0.1161	0.3101	0.0311	0.0303
	12	43.7241	46.5987	47.3371	44.9737	48.0974	48.2165	0.0957	0.1399	0.2230	0.0500	0.0278	0.0278

Table 2 continued

Test Images	m	Best objective values						ME					
		BAT	PSO	WDO	MBO	GOA	WCA	BAT	PSO	WDO	MBO	GOA	WCA
IMG6	3	24.1001	24.3211	24.3169	24.1788	24.3219	24.3217	0.5472	0.5830	0.5625	0.5484	0.5858	0.5843
	5	31.1547	31.9538	31.9820	31.4907	32.0148	31.9846	0.3254	0.4799	0.5117	0.5147	0.4984	0.4974
	8	40.0675	41.1692	41.2524	40.7387	41.4379	41.2775	0.3885	0.4184	0.4442	0.4383	0.4295	0.4209
	12	49.4834	50.4927	51.1964	48.9085	51.2882	51.0154	0.2568	0.3315	0.4337	0.3829	0.4044	0.3976
IMG7	3	23.3164	23.4230	23.4276	23.0121	23.4276	23.4276	0.6154	0.5047	0.5009	0.6136	0.4978	0.4978
	5	29.9767	30.2605	30.2963	29.9847	30.2986	30.2841	0.3824	0.3555	0.3672	0.3155	0.3537	0.3530
	8	37.4742	38.0977	38.4448	36.9008	38.5395	38.3252	0.2659	0.2503	0.3129	0.3515	0.2536	0.2291
	12	41.1657	45.8514	47.0507	41.1935	47.1958	46.8605	0.1607	0.1737	0.1995	0.2498	0.1882	0.1391
IMG8	3	23.5163	24.0351	23.8610	23.6665	24.0208	24.0520	0.0425	0.0291	0.0442	0.0299	0.0238	0.0308
	5	30.1625	31.4701	31.4361	31.0079	31.4722	31.5756	0.0249	0.0101	0.0149	0.0120	0.0184	0.0119
	8	38.6747	39.7974	40.2670	38.9761	40.4634	40.4327	0.0092	0.0053	0.0071	0.0094	0.0060	0.0048
	12	48.0959	48.8381	49.6706	46.8829	49.6887	49.6197	0.0056	0.0019	0.0046	0.0059	0.0051	0.0023
IMG9	3	25.0622	25.1968	25.1974	25.0745	25.1998	25.1990	0.3627	0.3313	0.3382	0.1342	0.3172	0.3118
	5	32.2101	32.8962	32.9332	32.4852	32.9338	32.9339	0.2004	0.1223	0.1164	0.0941	0.1111	0.1111
	8	40.4392	41.8573	42.1557	41.5616	42.2111	42.1812	0.1027	0.0913	0.0835	0.0875	0.0784	0.0740
	12	49.9727	50.9584	51.7581	50.1221	52.1058	51.9546	0.9624	0.0466	0.0666	0.0449	0.0402	0.0385
IMG10	3	24.1035	24.3549	24.2254	24.2075	24.3568	24.3566	0.3499	0.3455	0.2054	0.4106	0.3476	0.3476
	5	30.8900	31.4720	31.5701	31.1903	31.5722	31.4965	0.2498	0.1517	0.1552	0.1582	0.1684	0.1486
	8	39.2608	39.9224	40.2683	39.2633	40.4068	40.1706	0.0998	0.0950	0.0732	0.0282	0.0708	0.0259
	12	48.1145	48.3231	49.6991	46.7666	49.7289	49.7500	0.0339	0.0339	0.0321	0.0289	0.0346	0.0214

Table 3 Comparison of best objective values (entropy) and ME computed by different algorithms using Masi entropy

Test Images	m	Best objective values						ME					
		BAT	PSO	WDO	MBO	GOA	WCA	BAT	PSO	WDO	MBO	GOA	WCA
IMG1	3	26.6810	27.4789	27.2242	27.1595	27.2242	27.4859	0.3456	0.4148	0.4240	0.4245	0.4167	0.4167
	5	33.6287	33.9236	33.9193	33.3791	33.9986	33.7726	0.2393	0.1384	0.2867	0.1929	0.1532	0.1384
	8	34.4078	41.9836	42.3678	41.4078	42.3893	42.1377	0.0882	0.1111	0.1475	0.1086	0.1018	0.0873
	12	47.9780	50.5366	51.2376	50.0426	51.3765	52.5470	0.0598	0.0904	0.1413	0.0853	0.0871	0.0537
IMG2	3	25.1811	25.3319	25.3338	25.2388	25.3337	25.3339	0.2709	0.2753	0.2664	0.2671	0.2741	0.2608
	5	30.1201	31.3222	31.3330	31.1011	31.3620	31.3663	0.1444	0.1467	0.1499	0.1691	0.1446	0.1405
	8	38.2523	38.5286	38.8355	37.9862	38.9740	38.8282	0.1044	0.0496	0.0686	0.0219	0.0499	0.0179
	12	44.2169	45.9221	46.9592	45.3514	46.4144	47.2531	0.0146	0.0438	0.0356	0.0164	0.0417	0.0092
IMG3	3	27.0690	27.2621	27.3025	27.2844	27.1133	27.3035	0.2691	0.2629	0.2513	0.2628	0.2195	0.2190
	5	33.1745	34.0943	33.8430	33.8468	34.2392	34.1157	0.1275	0.1245	0.1294	0.1185	0.1219	0.1132
	8	41.8906	42.2943	42.1705	41.7210	42.7027	42.7085	0.0929	0.1075	0.1015	0.0883	0.0981	0.0867
	12	48.7221	50.3378	51.1508	49.0052	51.1461	51.0335	0.0720	0.0503	0.0734	0.0282	0.0659	0.0272
IMG4	3	24.0474	24.3120	24.3200	24.3103	24.3594	24.3195	0.2865	0.2896	0.2928	0.2848	0.3348	0.2803
	5	29.5679	30.5902	30.7264	30.5064	30.8314	30.6697	0.1986	0.1598	0.1848	0.1278	0.2634	0.1205
	8	37.2637	38.0770	37.6447	37.9510	38.3390	38.4531	0.0551	0.0358	0.0627	0.0335	0.0346	0.0332
	12	43.5186	45.8086	46.6270	44.4961	46.5681	45.7637	0.0168	0.0194	0.0176	0.0168	0.0201	0.0123
IMG5	3	26.1574	26.2372	26.2482	26.2123	26.2519	26.2589	0.6598	0.6205	0.6224	0.6071	0.6259	0.6201
	5	31.6403	32.6291	32.7057	32.6483	32.6981	32.7331	0.2726	0.2500	0.4602	0.4260	0.2418	0.2402
	8	39.2784	40.4329	40.6107	40.2742	40.8125	40.7968	0.0450	0.2545	0.1204	0.1693	0.1377	0.0363
	12	47.0336	48.5701	48.9930	47.9102	49.5631	49.4614	0.0149	0.0036	0.2367	0.0383	0.0003	0.0002

Table 3 continued

Test Images	m	Best objective values						ME					
		BAT	PSO	WDO	MBO	GOA	WCA	BAT	PSO	WDO	MBO	GOA	WCA
IMG6	3	27.4615	28.0444	28.0507	27.9091	28.0509	28.0516	0.5429	0.5450	0.5419	0.5490	0.5414	0.5385
	5	34.6827	35.1996	35.1593	34.8721	35.1654	35.1626	0.4845	0.4523	0.4557	0.4684	0.4474	0.4474
	8	40.3257	43.7379	44.0565	43.4377	44.1106	44.0160	0.4249	0.3986	0.4378	0.4362	0.4177	0.4162
	12	52.2337	52.7060	53.1992	51.9110	53.2519	53.2351	0.3847	0.3570	0.4133	0.3435	0.3894	0.3425
IMG7	3	26.7832	26.5221	26.5233	26.4987	26.5256	26.5256	0.5960	0.4896	0.4972	0.5096	0.4887	0.4887
	5	33.0155	32.8431	32.8819	32.7158	32.8823	32.8806	0.3800	0.3717	0.3670	0.3643	0.3561	0.3511
	8	39.0899	40.2794	40.5465	39.8385	40.5075	40.5660	0.2601	0.2376	0.3037	0.2619	0.2761	0.2513
	12	45.4787	47.9411	47.9221	45.7391	48.6288	48.5744	0.1552	0.1335	0.3088	0.1570	0.1568	0.1513
IMG8	3	27.7280	27.1908	27.4399	27.3665	27.4013	27.3773	0.0246	0.0422	0.0458	0.0242	0.0492	0.0406
	5	33.2309	34.2908	34.2769	33.7945	34.4285	34.2825	0.0229	0.0117	0.0180	0.0153	0.0116	0.0162
	8	41.8751	42.3056	42.6670	41.8956	42.6795	42.6635	0.0027	0.0032	0.0081	0.0023	0.0034	0.0031
	12	50.2470	50.0783	51.5005	50.0429	51.4546	51.4045	0.0087	0.0023	0.0048	0.0034	0.0026	0.0020
IMG9	3	29.2846	29.3033	29.3062	29.2946	29.3067	29.3067	0.1228	0.1269	0.1467	0.1284	0.1269	0.1206
	5	20.1897	36.4456	36.4737	36.2666	36.4759	36.4743	0.0871	0.1092	0.1189	0.1528	0.0811	0.0801
	8	44.2452	44.7442	45.0135	44.3202	45.0497	45.0507	0.0618	0.0898	0.0807	0.0789	0.0709	0.0591
	12	53.6070	53.3127	54.0538	52.4540	54.0444	54.0928	0.0576	0.0467	0.0821	0.0454	0.0310	0.0307
IMG10	3	27.7508	27.8115	27.7321	27.7441	27.5486	27.8170	0.3513	0.3460	0.1835	0.3599	0.1740	0.1476
	5	34.3078	34.2824	34.4133	34.0951	34.3000	34.3048	0.0882	0.1051	0.1694	0.1258	0.1507	0.0817
	8	42.3127	42.1838	42.3750	41.7415	42.5671	42.5470	0.0241	0.0658	0.0728	0.0299	0.0451	0.0207
	12	50.3471	50.2649	51.1724	49.4832	51.3857	51.4777	0.0194	0.0201	0.0273	0.0087	0.0279	0.0073

Table 4 Comparison of MSE and PSNR computed by different algorithms using Tsallis entropy

Test Images	m	MSE						PSNR					
		BAT	PSO	WDO	MBO	GOA	WCA	BAT	PSO	WDO	MBO	GOA	WCA
IMG1	3	2329.117	1657.781	1592.075	1657.840	1658.782	1651.283	14.4588	15.9355	16.1111	15.9353	15.9329	15.9525
	5	966.3367	646.6796	750.4083	506.9183	632.8722	483.6508	18.2795	20.0239	19.3778	21.0814	20.1176	21.2854
	8	597.2589	257.6861	231.4519	715.3292	231.6539	204.8888	20.3691	24.0198	24.4861	19.5857	24.4824	25.0156
	12	246.0013	132.4347	145.5454	185.6143	178.5549	126.0360	24.2214	26.9107	26.5008	25.4446	25.6130	27.1258
IMG2	3	2477.346	1872.570	1827.429	1609.604	1844.907	1844.762	14.1909	15.4064	15.5123	16.0636	15.4710	15.4713
	5	2812.490	773.8249	1047.408	930.7994	749.3698	747.4913	13.6398	19.2443	17.9296	18.4422	19.3838	19.3947
	8	529.9086	247.4238	401.5091	446.4363	404.6433	224.3851	20.8887	24.1963	22.0938	21.6332	22.0600	24.6208
	12	251.1864	134.1501	103.6165	228.6657	131.5480	94.9620	24.1308	26.8548	27.9765	24.5387	26.9399	28.3553
IMG3	3	4610.765	2163.111	1756.611	1265.359	1157.106	1156.930	11.4930	14.7800	15.6840	17.1086	17.4970	17.4977
	5	3409.098	845.0531	613.2652	695.0360	759.1298	714.7138	12.8044	18.8619	20.2543	19.7107	19.3276	19.5894
	8	558.9698	379.2637	274.1164	321.8267	311.0264	252.4922	20.6569	22.3413	23.7514	23.0545	23.2028	24.1083
	12	494.7088	167.8417	207.1465	212.0112	157.3247	129.9917	21.1873	25.8818	24.9680	24.8672	26.1628	26.9916
IMG4	3	2999.194	2208.992	2179.095	2244.713	3095.866	2167.387	13.3607	14.6888	14.7480	14.6191	13.2229	14.7714
	5	2043.011	1473.985	1552.021	1176.138	1864.624	578.3216	15.0280	16.4458	16.2218	17.4262	15.4248	23.9410
	8	672.9349	445.6058	721.6192	337.6573	292.6481	262.4043	19.8510	21.6412	19.5477	22.8460	23.4673	20.5091
	12	293.9376	185.0830	132.2968	237.5685	168.8779	127.8007	23.4482	25.4571	26.9153	24.3729	25.8550	27.0654
IMG5	3	2032.603	2178.213	2216.885	2488.122	2193.867	2173.083	15.0502	14.7497	14.6733	14.1720	14.7186	14.7600
	5	1635.736	1348.851	1347.347	1283.824	1309.381	1280.253	15.9936	16.8311	16.8360	17.0457	16.9601	22.7945
	8	450.2605	817.4483	427.3445	735.1722	388.4176	341.6838	21.5961	19.0062	21.8230	19.4669	22.2378	17.0578
	12	308.8621	319.8442	473.5711	327.1159	217.2874	192.0187	23.2331	23.0814	21.3769	22.9837	24.7604	25.2973

Table 4 continued

Test Images	m	MSE						PSNR					
		BAT	PSO	WDO	MBO	GOA	WCA	BAT	PSO	WDO	MBO	GOA	WCA
IMG6	3	987.0456	830.2028	829.7392	901.0295	830.1584	829.6667	18.1874	18.9389	18.9413	18.5834	18.9391	18.9417
	5	538.0868	373.6915	397.4516	579.3526	436.8545	377.2228	20.8222	22.4056	22.1379	20.5013	21.7274	22.3648
	8	308.5379	204.9673	207.8084	279.2073	190.3819	186.0385	23.2377	25.0139	24.9541	23.6715	25.3345	25.4347
	12	198.7499	141.5556	129.1789	161.8157	126.0390	115.0182	25.1477	26.6215	27.0188	26.0405	27.1257	27.5231
IMG7	3	695.2308	711.5475	710.0882	1250.853	704.0629	704.0629	19.7095	19.6087	19.6176	17.1587	19.6546	19.6546
	5	355.8365	355.0479	350.2766	363.6682	346.3414	343.9169	22.6182	22.6279	22.6866	22.5237	22.7357	22.7662
	8	569.8280	183.5467	209.9983	390.1004	163.5987	161.9772	20.5733	25.4933	24.9086	22.2190	25.9930	26.0362
	12	358.0817	103.5121	98.6003	302.0821	93.1860	81.5990	22.5909	27.9808	28.1920	23.3295	28.4372	29.0139
IMG8	3	2676.075	1415.517	1155.465	1410.582	1376.921	1361.884	13.8558	16.6216	17.5032	16.6368	16.7417	16.7894
	5	1273.115	862.1839	657.3221	720.5909	802.3219	761.9887	17.0821	18.7748	19.9530	19.5539	19.0873	19.3113
	8	1119.215	371.4364	292.1027	347.9131	291.0752	286.2890	17.6416	22.4319	23.4754	22.7160	23.4907	23.5627
	12	246.4926	215.8021	161.8803	185.3232	171.9952	139.5100	24.2127	24.7902	26.0388	25.4515	25.7756	26.6847
IMG9	3	1538.622	1546.127	1512.029	1415.415	1508.786	1404.460	16.2594	16.2383	16.3352	16.6219	16.3445	16.6557
	5	1295.339	595.3676	582.8319	710.3856	571.1262	566.8527	17.0069	20.3829	20.4753	19.6158	20.5634	20.5961
	8	991.9354	310.3972	274.5883	323.1550	275.9448	272.0461	18.1659	23.2116	23.7439	23.0366	23.7225	23.7843
	12	328.8292	211.8525	178.1365	198.9144	126.4611	123.5397	22.9610	24.8704	25.6232	25.1441	27.1112	27.2127
IMG10	3	3853.107	1920.841	1453.017	2217.726	1916.256	1913.173	12.2726	15.2958	16.5080	14.6717	15.3062	15.3132
	5	1032.793	756.5383	836.2672	848.2029	829.2271	747.2794	17.9906	19.3424	18.9073	18.8458	18.9440	19.3959
	8	429.2603	373.0270	322.7719	499.6533	325.1023	264.6941	21.8035	22.4134	23.0418	21.1441	23.0106	23.9033
	12	237.4513	184.4520	149.7612	261.4616	154.8862	119.8224	24.3750	25.4719	26.3768	23.9567	26.2306	27.3454

Table 5 Comparison of MSE and PSNR computed by different algorithms using Masi entropy

Test Images	m	MSE						PSNR					
		BAT	PSO	WDO	MBO	GOA	WCA	BAT	PSO	WDO	MBO	GOA	WCA
IMG1	3	1907.897	1659.598	1206.761	1194.943	1166.368	1658.454	15.3252	15.9307	17.3145	17.3573	17.4624	15.9337
	5	582.3666	547.8266	723.4511	503.7277	488.2661	385.5977	20.4788	20.7443	19.5367	21.1088	21.2442	22.2694
	8	775.0387	243.5058	229.1289	337.3675	191.8945	179.6851	19.2375	24.2657	24.5300	22.8497	25.3001	25.5856
	12	156.888	105.4432	141.5649	169.5977	116.8384	109.9004	26.1749	27.9006	26.6212	25.8366	27.4549	27.7208
IMG2	3	1994.531	1860.240	1778.729	1790.225	1840.429	1667.177	15.1323	15.4351	15.6297	15.6017	15.4816	15.9109
	5	1024.982	737.1750	754.2279	831.5745	737.0215	717.8710	18.0236	19.4550	19.3557	18.9317	19.4560	19.5703
	8	402.7459	237.5100	266.9797	259.9666	220.4617	211.1958	22.0804	24.3739	23.8660	23.9816	24.6974	24.8839
	12	153.5339	125.5113	110.1747	197.4294	114.5827	105.0374	26.2687	27.1439	27.7099	25.1766	27.5396	27.9173
IMG3	3	1781.675	1595.124	1570.839	1588.655	1138.436	1569.627	15.6225	16.1028	16.1694	16.1205	17.5677	16.1728
	5	1166.486	751.4732	588.9525	687.1949	624.3157	616.7650	17.4620	19.3716	20.4300	19.7600	20.1767	20.2296
	8	398.7838	336.1622	265.1657	278.3702	290.5861	263.2799	22.1234	22.8653	23.8956	23.6845	23.4980	23.9266
	12	256.3238	143.4300	170.4635	181.1443	155.9730	131.3008	24.0429	26.5644	25.8144	25.5505	26.2003	26.9481
IMG4	3	2645.895	2188.003	2150.925	2158.003	2694.728	2131.081	13.9050	14.7303	14.8045	14.7902	13.8256	14.8448
	5	1727.866	1374.457	1328.548	1125.023	1656.627	801.7596	15.7557	16.7494	16.8970	17.6191	15.9385	19.0903
	8	375.1304	273.6131	324.2423	286.7381	271.1008	229.9580	22.3889	23.7594	23.0221	23.5559	23.7994	24.5143
	12	276.1277	156.0622	119.4704	172.3331	136.8360	109.8640	23.7197	26.1978	27.3582	25.7671	26.7687	27.7222
IMG5	3	2440.744	2166.883	2202.042	2090.797	2218.364	2194.301	14.2555	14.7724	14.7025	14.9276	14.6704	14.7178
	5	880.9027	1051.734	1284.765	1169.207	1026.750	1014.176	18.6815	17.9117	17.0425	17.4518	18.0161	18.0696
	8	405.4003	574.8633	415.9868	611.7878	496.1246	355.3255	22.0519	20.5351	21.9400	20.2647	21.1748	22.6245
	12	251.3370	173.3319	469.3152	274.5418	120.8373	105.5106	24.1282	25.7420	21.4161	23.7447	27.3087	27.8978

Table 5 continued

Test Images	m	MSE						PSNR					
		BAT	PSO	WDO	MBO	GOA	WCA	BAT	PSO	WDO	MBO	GOA	WCA
IMG6	3	1952.355	947.8553	933.7278	858.8974	940.0461	938.9922	15.2252	18.3633	18.4286	18.7913	18.3993	18.4041
	5	486.1624	452.7884	379.5472	447.6889	405.5670	383.4907	21.2629	21.5718	22.3381	21.6210	22.0501	22.2932
	8	267.9626	207.4237	205.4541	208.7744	200.6867	193.1228	23.8500	24.9622	25.0036	24.9340	25.1056	25.2724
	12	150.6573	131.2338	123.5594	155.2184	111.5679	107.8503	26.3509	26.9503	27.2120	26.2213	27.6554	27.8025
IMG7	3	943.3454	698.3214	709.2467	717.6921	703.9962	703.9962	18.3840	19.6902	19.6228	19.5714	19.6551	19.6551
	5	477.7652	338.8332	348.8553	348.3117	355.3824	350.3098	21.3386	22.8309	22.7043	22.7111	22.6238	22.6862
	8	260.2893	178.9940	205.6641	208.3290	192.9579	164.2313	23.9762	25.6024	24.9992	24.9433	25.2761	25.9762
	12	177.9725	93.7994	201.5786	123.2034	82.6243	80.9288	25.6272	28.4088	25.0863	27.2245	28.9597	29.0497
IMG8	3	1658.768	1238.750	1153.625	1405.235	1140.479	1139.377	15.9329	17.2009	17.5101	16.6533	17.5599	17.5641
	5	536.6176	833.4880	621.4000	608.6535	673.0879	605.6759	20.8341	18.9218	20.1970	20.2871	19.8500	20.3084
	8	315.1776	351.2660	276.7228	302.4039	271.2235	264.2881	23.1452	22.6744	23.7103	23.3249	23.7975	23.9100
	12	162.7694	168.7567	143.8844	137.0611	147.1909	140.3064	26.0150	25.8581	26.5506	26.7616	26.4519	26.6600
IMG9	3	1301.492	1254.169	1183.938	1240.940	1236.931	1205.920	16.9863	17.1472	17.3975	17.1932	17.2073	17.3176
	5	637.4961	574.7344	564.1440	597.7608	567.3688	561.5978	20.0860	20.5361	20.6169	20.3655	20.5921	20.6365
	8	322.5220	282.9169	269.7142	314.9966	272.4066	264.5908	23.0452	23.6142	23.8217	23.1477	23.7786	23.9050
	12	199.7894	164.0251	159.8043	186.6064	132.8069	128.9092	25.1250	25.9817	26.0949	25.4215	26.8985	27.0279
IMG10	3	2163.980	1914.501	1472.855	2007.900	1281.432	1921.749	14.7782	15.3102	16.4492	15.1033	17.0538	15.2938
	5	775.0387	694.3670	827.7491	745.8902	729.7852	626.8542	19.2375	19.7149	18.9518	19.4040	19.4988	20.1591
	8	363.3477	301.1411	317.1194	336.9517	310.4724	290.9004	22.5275	23.3431	23.1185	22.8551	23.2105	23.4933
	12	243.0949	150.2649	138.4998	203.3034	142.9496	133.3641	24.2730	26.3622	26.7163	25.0493	26.5789	26.8804

Table 6 Comparison of SSIM and FSIM computed by different algorithms using Tsallis entropy

Test Images	m	SSIM						FSIM					
		BAT	PSO	WDO	MBO	GOA	WCA	BAT	PSO	WDO	MBO	GOA	WCA
IMG1	3	0.9245	0.9467	0.9452	0.9523	0.9466	0.9468	0.7885	0.8155	0.8122	0.8016	0.8156	0.8156
	5	0.9690	0.9788	0.9738	0.9847	0.9787	0.9852	0.8248	0.8587	0.8430	0.8611	0.8656	0.8714
	8	0.9797	0.9919	0.9925	0.9878	0.9928	0.9936	0.8397	0.8702	0.8791	0.8490	0.8838	0.8860
	12	0.9921	0.9960	0.9951	0.9941	0.9940	0.9979	0.8645	0.9014	0.8847	0.8750	0.8981	0.8996
IMG2	3	0.9280	0.9452	0.9466	0.9557	0.9460	0.9467	0.7843	0.8032	0.8037	0.7945	0.8033	0.8039
	5	0.9160	0.9770	0.9678	0.9749	0.9774	0.9774	0.7902	0.8611	0.8584	0.8358	0.8689	0.8699
	8	0.9876	0.9932	0.9876	0.9884	0.9875	0.9939	0.8870	0.9290	0.9134	0.8803	0.9164	0.9418
	12	0.9935	0.9965	0.9974	0.9944	0.9972	0.9976	0.9242	0.9607	0.9681	0.9212	0.9619	0.9767
IMG3	3	0.8681	0.9377	0.9477	0.9624	0.9667	0.9667	0.6128	0.7861	0.8050	0.8188	0.8294	0.8288
	5	0.9016	0.9748	0.9722	0.9801	0.9780	0.9795	0.6780	0.8664	0.8612	0.8663	0.8682	0.8741
	8	0.9848	0.9892	0.9918	0.9907	0.9908	0.9926	0.8779	0.9188	0.9339	0.9213	0.9302	0.9385
	12	0.9839	0.9952	0.9935	0.9939	0.9952	0.9964	0.8884	0.9547	0.9482	0.9436	0.9595	0.9649
IMG4	3	0.9302	0.9352	0.9363	0.9353	0.9074	0.9419	0.6684	0.7140	0.7122	0.7126	0.6810	0.6915
	5	0.9407	0.9561	0.9503	0.9635	0.9400	0.9856	0.6965	0.7754	0.7709	0.7737	0.7534	0.7675
	8	0.9790	0.9860	0.9760	0.9912	0.9917	0.9929	0.7913	0.8290	0.8262	0.8384	0.8532	0.8644
	12	0.9922	0.9953	0.9967	0.9938	0.9954	0.9975	0.8481	0.8912	0.9147	0.8768	0.9049	0.9152
IMG5	3	0.9315	0.9232	0.9218	0.9134	0.9226	0.9233	0.7884	0.8004	0.8005	0.7848	0.8027	0.8033
	5	0.9404	0.9505	0.9504	0.9528	0.9518	0.9529	0.8396	0.8530	0.8575	0.8587	0.8595	0.8636
	8	0.9860	0.9693	0.9844	0.9729	0.9901	0.9880	0.8692	0.8772	0.9180	0.8765	0.9165	0.9212
	12	0.9897	0.9882	0.9820	0.9883	0.9923	0.9931	0.9185	0.9138	0.9142	0.9097	0.9506	0.9542

Table 6 continued

Test Images	m	SSIM						FSIM					
		BAT	PSO	WDO	MBO	GOA	WCA	BAT	PSO	WDO	MBO	GOA	WCA
IMG6	3	0.9709	0.9762	0.9758	0.9753	0.9761	0.9762	0.7585	0.7840	0.7897	0.7794	0.7843	0.7843
	5	0.9848	0.9880	0.9878	0.9842	0.9872	0.9883	0.8236	0.8537	0.8514	0.8225	0.8450	0.8542
	8	0.9898	0.9936	0.9934	0.9914	0.9940	0.9944	0.8699	0.9133	0.9142	0.8896	0.9197	0.9200
	12	0.9940	0.9955	0.9956	0.9950	0.9957	0.9961	0.9055	0.9355	0.9449	0.9189	0.9514	0.9524
IMG7	3	0.9752	0.9751	0.9752	0.9567	0.9755	0.9755	0.7859	0.7928	0.7954	0.7484	0.7957	0.7957
	5	0.9882	0.9874	0.9875	0.9873	0.9877	0.9878	0.8728	0.8757	0.8755	0.8719	0.8798	0.8788
	8	0.9905	0.9934	0.9922	0.9859	0.9942	0.9943	0.8075	0.9222	0.9153	0.8586	0.9336	0.9351
	12	0.9985	0.9963	0.9964	0.9897	0.9966	0.9971	0.8649	0.9492	0.9528	0.8833	0.9570	0.9656
IMG8	3	0.9442	0.9760	0.9689	0.9760	0.9764	0.9767	0.7290	0.8322	0.8142	0.8120	0.8259	0.8322
	5	0.9762	0.9856	0.9862	0.9870	0.9866	0.9873	0.7888	0.8552	0.8434	0.8429	0.8491	0.8605
	8	0.9784	0.9937	0.9947	0.9935	0.9946	0.9948	0.7841	0.8709	0.8805	0.8678	0.8804	0.8819
	12	0.9947	0.9960	0.9972	0.9963	0.9968	0.9973	0.8918	0.8967	0.9127	0.9096	0.9119	0.9172
IMG9	3	0.9568	0.9530	0.9537	0.9600	0.9544	0.9555	0.7810	0.8119	0.8059	0.7937	0.8115	0.8144
	5	0.9635	0.9825	0.9829	0.9801	0.9835	0.9836	0.7975	0.9043	0.9080	0.8806	0.9098	0.9102
	8	0.9706	0.9906	0.9921	0.9903	0.9917	0.9919	0.8311	0.9457	0.9574	0.9452	0.9587	0.9600
	12	0.9908	0.9938	0.9944	0.9938	0.9964	0.9965	0.9475	0.9622	0.9707	0.9551	0.9836	0.9843
IMG10	3	0.9004	0.9442	0.9425	0.9331	0.9441	0.9441	0.6718	0.7514	0.7502	0.7450	0.7518	0.7518
	5	0.9745	0.9782	0.9752	0.9756	0.9751	0.9787	0.7728	0.8208	0.8213	0.8109	0.8217	0.8217
	8	0.9901	0.9886	0.9911	0.9852	0.9907	0.9935	0.8338	0.8639	0.8808	0.8564	0.8819	0.8862
	12	0.9936	0.9951	0.9960	0.9942	0.9955	0.9970	0.8885	0.9085	0.9262	0.8869	0.9295	0.9393

Table 7 Comparison of SSIM and FSIM computed by different algorithms using Masi method

Test Images	m	SSIM						FSIM					
		BAT	PSO	WDO	MBO	GOA	WCA	BAT	PSO	WDO	MBO	GOA	WCA
IMG1	3	0.9401	0.9468	0.9600	0.9606	0.9617	0.9469	0.8001	0.8156	0.8258	0.8238	0.8259	0.8269
	5	0.9815	0.9829	0.9758	0.9849	0.9851	0.9883	0.8379	0.8742	0.8515	0.8255	0.8730	0.8733
	8	0.9790	0.9922	0.9928	0.9897	0.9941	0.9947	0.8108	0.8753	0.8749	0.8739	0.8863	0.8858
	12	0.9951	0.9968	0.9953	0.9945	0.9963	0.9989	0.8717	0.8946	0.8948	0.8915	0.9012	0.9055
IMG2	3	0.9425	0.9459	0.9485	0.9477	0.9464	0.9486	0.7935	0.8033	0.8035	0.7972	0.8038	0.8042
	5	0.9694	0.9785	0.9778	0.9745	0.9783	0.9789	0.8382	0.8658	0.8664	0.8514	0.8679	0.8684
	8	0.9883	0.9937	0.9924	0.9937	0.9945	0.9946	0.8961	0.9334	0.9254	0.9287	0.9400	0.9423
	12	0.9961	0.9968	0.9972	0.9943	0.9969	0.9980	0.9501	0.9639	0.9681	0.9311	0.9725	0.9778
IMG3	3	0.9519	0.9546	0.9558	0.9543	0.9671	0.9674	0.7914	0.7935	0.8000	0.8004	0.8219	0.8295
	5	0.9673	0.9791	0.9834	0.9812	0.9827	0.9829	0.8458	0.8789	0.8801	0.8750	0.8811	0.8832
	8	0.9880	0.9898	0.9920	0.9916	0.9914	0.9929	0.9188	0.9221	0.9315	0.9323	0.9305	0.9357
	12	0.9923	0.9959	0.9950	0.9945	0.9953	0.9972	0.9338	0.9618	0.9553	0.9512	0.9612	0.9664
IMG4	3	0.9256	0.9362	0.9364	0.9369	0.9213	0.9469	0.6790	0.7154	0.7095	0.7127	0.7082	0.7195
	5	0.9468	0.9586	0.9592	0.9671	0.9478	0.9865	0.7402	0.7758	0.7765	0.7721	0.7706	0.7884
	8	0.9909	0.9923	0.9918	0.9922	0.9927	0.9939	0.8348	0.8574	0.8454	0.8533	0.8606	0.8714
	12	0.9929	0.9959	0.9969	0.9956	0.9965	0.9975	0.8671	0.9013	0.9190	0.8924	0.9123	0.9270
IMG5	3	0.9145	0.9237	0.9224	0.9261	0.9219	0.9287	0.7747	0.8036	0.8017	0.8033	0.8000	0.8039
	5	0.9703	0.9644	0.9528	0.9573	0.9631	0.9656	0.8522	0.8559	0.8632	0.8597	0.8697	0.8703
	8	0.9866	0.9788	0.9849	0.9776	0.9820	0.9895	0.9052	0.8914	0.9098	0.8892	0.9052	0.9323
	12	0.9912	0.9942	0.9820	0.9901	0.9961	0.9966	0.9307	0.9599	0.9168	0.9329	0.9764	0.9806

Table 7 continued

Test Images	m	SSIM						FSIM					
		BAT	PSO	WDO	MBO	GOA	WCA	BAT	PSO	WDO	MBO	GOA	WCA
IMG6	3	0.9495	0.9739	0.9740	0.9759	0.9741	0.9753	0.7359	0.7848	0.7843	0.7870	0.7853	0.7876
	5	0.9847	0.9868	0.9888	0.9873	0.9880	0.9890	0.8467	0.8472	0.8620	0.8495	0.8540	0.8587
	8	0.9919	0.9940	0.9934	0.9934	0.9937	0.9949	0.9013	0.9148	0.9127	0.9133	0.9143	0.9184
	12	0.9953	0.9959	0.9959	0.9951	0.9963	0.9969	0.9312	0.9409	0.9480	0.9274	0.9574	0.9577
IMG7	3	0.9666	0.9759	0.9754	0.9749	0.9756	0.9759	0.7455	0.7991	0.7960	0.7920	0.7982	0.7982
	5	0.9833	0.9879	0.9876	0.9877	0.9874	0.9886	0.8534	0.8763	0.8759	0.8753	0.8760	0.8792
	8	0.9911	0.9937	0.9924	0.9926	0.9930	0.9946	0.8917	0.9284	0.9185	0.9169	0.9254	0.9362
	12	0.9938	0.9966	0.9923	0.9958	0.9970	0.9978	0.9200	0.9549	0.9173	0.9440	0.9646	0.9659
IMG8	3	0.9711	0.9771	0.9770	0.9754	0.9778	0.9778	0.8159	0.8157	0.8013	0.8278	0.8388	0.8392
	5	0.9892	0.9861	0.9895	0.9888	0.9890	0.9892	0.8432	0.8588	0.8427	0.8470	0.8451	0.8471
	8	0.9934	0.9939	0.9950	0.9945	0.9951	0.9956	0.8815	0.8729	0.8781	0.8755	0.8812	0.8834
	12	0.9969	0.9967	0.9976	0.9974	0.9972	0.9979	0.9126	0.9083	0.9232	0.9252	0.9174	0.9178
IMG9	3	0.9645	0.9655	0.9677	0.9659	0.9662	0.9682	0.8078	0.8143	0.8223	0.8142	0.8174	0.8236
	5	0.9702	0.9834	0.9836	0.9821	0.9836	0.9838	0.8105	0.9078	0.9088	0.8964	0.9098	0.9111
	8	0.9912	0.9915	0.9925	0.9909	0.9920	0.9929	0.9415	0.9536	0.9592	0.9464	0.9591	0.9602
	12	0.9941	0.9951	0.9949	0.9945	0.9962	0.9969	0.9648	0.9723	0.9723	0.9696	0.9830	0.9852
IMG10	3	0.9381	0.9438	0.9623	0.9414	0.9680	0.9437	0.7425	0.7509	0.7502	0.7516	0.7604	0.7615
	5	0.9790	0.9809	0.9753	0.9787	0.9792	0.9841	0.8108	0.8202	0.8227	0.8157	0.8224	0.8297
	8	0.9906	0.9920	0.9911	0.9917	0.9914	0.9920	0.8575	0.8774	0.8829	0.8684	0.8826	0.8875
	12	0.9933	0.9959	0.9965	0.9948	0.9961	0.9975	0.8978	0.9204	0.9290	0.9110	0.9398	0.9403

Table 8 Comparison of entropy obtained by using different algorithms for each sample image

Test Images	m	Tsallis						Masi					
		BAT	PSO	WDO	MBO	GOA	WCA	BAT	PSO	WDO	MBO	GOA	WCA
IMG1	3	1.9422	2.1818	2.0008	2.1426	2.1799	2.1841	2.3799	2.1838	2.4193	2.3956	2.3894	2.3795
	5	2.8596	3.1280	2.8217	2.8930	3.0711	3.1943	3.0674	3.1898	2.9132	3.2783	3.1810	3.4653
	8	3.4118	3.7515	3.7336	3.1421	3.9023	3.9498	3.5278	3.8485	3.7724	3.6225	3.9303	3.9390
	12	4.0120	4.1843	3.9345	3.9301	4.2374	4.2899	4.4197	4.4042	4.2372	3.9842	4.3301	4.3901
IMG2	3	2.8538	2.9800	2.9852	2.9712	2.9830	2.9852	2.9919	2.9850	2.9902	3.0089	2.9881	2.9882
	5	3.3284	3.6817	3.6641	3.6018	3.6338	3.7327	3.7026	3.5651	3.6718	3.6239	3.7209	3.7372
	8	4.0388	4.3197	4.2429	4.1293	4.2852	4.4144	4.2188	4.3470	4.3318	4.3448	4.3296	4.3808
	12	4.5660	4.8632	4.8044	4.4154	4.7727	4.8868	4.6194	4.5330	4.8801	4.5952	4.8679	4.8895
IMG3	3	2.3741	2.2732	2.5199	2.3830	2.5393	2.5423	2.5703	2.5105	2.5265	2.5162	2.7657	2.5456
	5	2.9604	3.1777	3.1182	3.2159	3.1682	3.2239	3.2158	3.2691	3.3013	3.2882	3.3058	3.3108
	8	3.7628	3.7898	4.0479	3.3065	3.9616	4.1293	3.9196	3.9009	4.0128	3.4903	4.0204	4.0394
	12	4.1955	4.4984	4.3090	4.2109	4.4124	4.5608	4.4060	4.4868	4.4122	4.3840	4.5409	4.5733
IMG4	3	2.9187	2.9262	2.9478	2.9853	2.3984	2.9484	2.7696	2.9580	2.9573	2.9506	2.7474	2.9575
	5	3.2990	3.5075	3.4257	3.5937	3.1778	3.4438	3.3467	3.5738	3.5465	3.5406	3.3981	3.5932
	8	4.0849	4.1796	4.2000	4.0410	4.2036	4.2235	4.1295	4.2723	4.2120	4.0714	4.2387	4.2839
	12	4.3088	4.5967	4.6241	4.4790	4.6651	4.6739	4.3951	4.6798	4.6811	4.6021	4.6732	4.7601
IMG5	3	1.9236	1.9329	1.8482	1.7365	1.9279	1.9425	1.7565	1.8988	1.8628	1.9834	1.8559	1.8720
	5	2.1226	2.6362	2.6439	2.5835	2.6309	2.7151	3.1996	3.0799	2.7174	2.8069	3.0296	3.0864
	8	3.2516	3.2573	3.7160	3.4405	3.8128	3.8506	3.4600	3.4473	3.6425	3.5227	3.4989	3.7792
	12	3.8070	4.0997	4.0013	3.4760	4.0018	4.0698	3.9443	4.2096	4.0716	4.0789	4.3584	4.3595

Table 8 continued

Test Images	m	Tsallis						Masi					
		BAT	PSO	WDO	MBO	GOA	WCA	BAT	PSO	WDO	MBO	GOA	WCA
IMG6	3	1.8882	2.0809	2.0614	1.9854	2.0827	2.0882	2.2350	2.2061	2.2218	2.1973	2.2233	2.2364
	5	2.6701	2.7176	2.6977	2.5088	2.6890	2.7500	2.7567	2.8339	2.8891	2.7367	2.9050	2.9582
	8	2.8529	3.2919	3.2706	2.5831	3.3367	3.3940	3.3327	3.4061	3.2927	3.0933	3.3595	3.3816
	12	3.7973	3.6368	3.5439	3.6197	3.6746	3.6863	3.7659	3.7995	3.6415	3.7318	3.8134	3.8341
IMG7	3	2.0502	2.2496	2.2341	1.7696	2.2744	2.2744	1.9175	2.3333	2.2841	2.0121	2.3075	2.3094
	5	2.5503	2.6626	2.8984	2.9334	2.9215	2.9898	3.0094	2.8083	2.7922	2.9846	2.9879	3.0113
	8	2.9939	3.6501	3.2606	2.9130	3.6112	3.8012	3.6771	3.7130	3.4079	3.3774	3.6227	3.7384
	12	3.8763	4.3077	4.1894	3.5902	4.2274	4.4705	4.0807	4.1718	3.6762	4.2892	4.2876	4.3807
IMG8	3	2.3589	2.5167	2.4674	2.0374	2.4684	2.5341	2.5033	2.6574	2.7615	2.5249	2.7313	2.7646
	5	2.8176	2.8599	3.0978	2.9846	2.9370	2.9425	3.1392	2.9088	3.1426	3.1766	3.1204	3.1443
	8	2.9354	3.5490	3.7403	3.6087	3.6964	3.7058	3.7641	3.5663	3.8517	3.4546	3.8097	3.7535
	12	3.9459	4.0187	4.0771	3.1308	3.8809	4.0814	4.0785	4.2344	4.2212	4.1823	4.2564	4.2819
IMG9	3	2.0989	2.8102	2.8111	2.2475	2.8469	2.8666	3.1278	3.0737	3.0934	3.0711	3.0932	3.1030
	5	3.4640	3.6144	3.5284	3.6288	3.5002	3.6511	3.7654	3.6650	3.5679	2.8701	3.5774	3.5782
	8	3.6468	4.1783	4.2835	4.0379	4.2420	4.2943	4.3116	4.2314	4.3069	4.2222	4.2620	4.3138
	12	4.4145	4.4858	4.6682	4.3004	4.9027	4.9423	4.4674	4.6532	4.6917	4.3856	4.8401	4.8519
IMG10	3	2.6599	2.6017	2.6237	2.6725	2.7444	2.7427	2.7045	2.7491	2.8597	2.7087	3.1567	2.7426
	5	3.5833	3.5738	3.5240	3.3134	3.4657	3.6130	3.5278	3.5485	3.5266	3.6117	3.6673	3.6860
	8	3.9873	4.2767	4.2026	3.8701	4.2786	4.3662	4.2144	4.3587	4.3902	4.1550	4.2350	4.3344
	12	4.6380	4.6900	4.6899	4.3264	4.7955	4.8357	4.6415	4.6819	4.7807	4.5147	4.7972	4.8629

Table 9 Comparison of CPU timing (seconds) obtained by using different algorithms for each sample image

| Test Images	m	Tsallis						Masi					
		BAT	PSO	WDO	MBO	GOA	WCA	BAT	PSO	WDO	MBO	GOA	WCA
IMG1	3	3.064241	2.042758	1.846648	1.132360	3.043941	2.172922	2.729718	1.886554	1.647181	1.133710	2.858181	1.560761
	5	3.127268	2.136245	1.917924	1.150149	3.596862	2.229018	2.864532	1.983129	1.698554	1.210767	3.347778	1.600512
	8	3.264451	2.217329	1.973822	1.266951	4.31361	2.314626	3.144932	2.114758	1.796637	1.376532	3.917079	1.693484
	12	3.629263	2.390708	2.157474	1.400572	5.208445	2.440397	3.011516	2.283915	1.943955	1.563293	4.998499	1.844940
IMG2	3	3.376751	2.323213	2.098434	1.415802	3.291224	2.543869	3.039097	2.290330	1.966063	1.425660	3.172987	1.651330
	5	3.593653	2.420012	2.246969	1.492039	3.871242	2.496350	3.173747	2.298351	2.065051	1.628909	3.680925	1.699563
	8	3.478856	2.551533	2.301698	1.590663	4.536667	2.514353	3.255377	2.431390	2.119484	1.711671	4.165527	1.810793
	12	3.692507	2.703696	2.421820	1.597828	5.418761	2.718983	3.524278	2.498293	2.157093	1.879737	5.276797	1.855314
IMG3	3	3.417266	2.456090	2.105522	1.414200	3.345031	2.415680	3.035354	2.153402	1.991174	1.424668	3.154539	1.697284
	5	3.496797	2.440508	2.212915	1.479021	3.937596	2.549610	3.241645	2.343459	2.024723	1.523116	3.703274	1.736053
	8	3.688308	2.578551	2.434279	1.548385	4.527138	2.657685	3.252934	2.412454	2.139619	1.695077	4.288098	1.869568
	12	3.940363	2.760373	2.511613	1.670923	5.681480	2.820902	3.422530	2.631573	2.271785	1.862901	5.403997	2.034918
IMG4	3	3.007738	1.961775	1.780454	1.038381	2.968650	2.078354	2.688919	1.831287	1.628306	1.071300	2.790454	1.333753
	5	3.105255	2.083076	1.896287	1.107947	3.520348	2.131320	2.741506	1.920795	1.662501	1.259352	3.321177	1.391788
	8	3.142912	2.162715	1.986756	1.197775	4.148654	2.280560	2.980492	2.091781	1.812234	1.323585	3.902595	1.486456
	12	3.324912	2.292093	2.118102	1.342651	5.207378	2.420468	2.998342	2.244436	1.941663	1.510050	4.997951	1.619551
IMG5	3	3.313723	2.341023	2.092476	1.410977	3.328259	2.446729	3.042230	2.202260	1.993396	1.388393	3.180866	1.783246
	5	3.415731	2.432804	2.172593	1.457714	3.850123	2.467152	3.111195	2.269911	2.086373	1.489396	3.700526	1.875028
	8	3.612044	2.545550	2.340386	1.587909	4.402758	2.548041	3.223933	2.507097	2.134811	1.690285	4.203067	1.909466
	12	3.902244	2.745547	2.404682	1.742962	5.550993	2.791429	3.267751	2.581133	2.163601	1.891578	5.252055	1.956325

Table 9 continued

Test Images	m	Tsallis						Masi					
		BAT	PSO	WDO	MBO	GOA	WCA	BAT	PSO	WDO	MBO	GOA	WCA
IMG6	3	3.560528	2.322217	2.121196	1.393874	3.296211	2.589151	3.051498	2.157469	1.930124	1.424629	3.139574	1.757205
	5	3.639132	2.442749	2.218921	1.441985	3.916344	2.534493	3.148693	2.258748	2.016930	1.596126	3.655890	1.913091
	8	3.587664	2.557660	2.343472	1.589342	4.472489	2.622218	3.368548	2.413964	2.120368	1.685067	4.208352	1.973476
	12	3.664967	2.648303	2.461953	1.722925	5.559611	2.870621	3.431996	2.627925	2.274186	1.792280	5.359747	2.075318
IMG7	3	3.462354	2.311418	2.106100	1.389536	3.313738	2.397093	3.145764	2.187313	1.949887	1.414667	3.102823	1.838840
	5	3.361374	2.420589	2.200434	1.454229	3.892024	2.476877	3.413669	2.287456	2.035837	1.517981	3.739177	1.949340
	8	3.524405	2.619137	2.307788	1.556151	4.441887	2.641374	3.298022	2.475883	2.130472	1.692463	4.240713	2.073395
	12	3.683715	2.705419	2.472781	1.734490	5.641763	2.742141	3.500602	2.658646	2.272981	1.902274	5.391924	2.261910
IMG8	3	3.445493	2.285896	2.171136	1.349684	3.369772	2.438821	3.107408	2.195035	1.957011	1.381983	3.168380	1.903105
	5	3.437417	2.339092	2.259347	1.410219	3.932368	2.475432	3.172579	2.322453	1.997903	1.484205	3.661069	2.022841
	8	3.460181	2.515218	2.281119	1.481569	4.431888	2.586342	3.100623	2.401727	2.160108	1.573004	4.172257	2.145962
	12	3.681267	2.667378	2.480032	1.657273	5.587312	2.883095	3.454415	2.573330	2.318785	1.843208	5.399538	2.188881
IMG9	3	3.361825	2.339379	2.126145	1.396423	3.348080	2.513841	3.231031	2.173848	2.021824	1.423619	3.117242	1.828056
	5	3.587134	2.414801	2.247124	1.453879	3.916358	2.487642	3.152700	2.366204	2.073128	1.524638	3.676654	2.071436
	8	3.555435	2.553502	2.293884	1.557555	4.457825	2.592829	3.199074	2.456286	2.093650	1.669190	4.225314	2.055384
	12	3.663386	2.841852	2.532738	1.851879	5.542501	2.769589	3.494165	2.605643	2.266900	1.848286	5.268247	2.169543
IMG10	3	3.485532	2.352906	2.131865	1.386404	3.329477	2.486543	3.046821	2.170185	1.939523	1.424374	3.149625	1.971243
	5	3.570638	2.424722	2.255303	1.495900	3.908645	2.446009	3.144932	2.247742	2.009180	1.521099	3.747954	1.980714
	8	3.739055	2.483903	2.317718	1.481708	4.464439	2.744119	3.214741	2.472509	2.073827	1.629913	4.273872	2.174626
	12	3.734478	2.652656	2.514762	1.775900	5.563878	2.772494	3.465809	2.612613	2.216497	1.835042	5.285317	2.369175

or nature; the best solution or result created at each run may not be same or identical. The complete analysis of the Tsallis-based optimization techniques has revealed that the WCA technique produces optimal value for a maximum number of fidelity parameters among all the techniques for almost every image. The objective function of Tsallis method is maximized to determine the thresholding results. The performance of different objective functions has been compared by using the quantitative results such as best objective function and ME values obtained by Tsallis which is reported in Table 2. Tables 4, 6, 8, and 9 depict the statistical evaluation of the quality parameters such as MSE, PSNR, SSIM, FSIM, entropy, and computational time, respectively. Figure 3 depicts the segmented results for all the images obtained at 3-level, 5-level, 8-level, and 12-level thresholding for each optimization algorithm (BAT, PSO, WDO, MBO, GOA, and WCA) (Fig. 4). Figures 5, 6, 7, 8, 9, and 10 show the plots of ME, MSE, PSNR, SSIM, FSIM, and entropy of 8-level MT using Tsallis entropy correspondingly, and it can be clearly noticed from the plots that the Tsallis-WCA method outperforms all other optimization (BAT, PSO, WDO, MBO, and GOA) techniques.

4.3 Experiment 2: Masi Entropy

In this section, several experimental results are reported using WCA, BAT, PSO, WDO, MBO, and GOA based on Masi entropy for multilevel color image thresholding segmentation. The ME and fitness function values using Masi entropy scheme are presented in Table 3. It has been tested that the misclassification error evaluated by the WCA coupled with Masi entropy harvests the lowest value among all the techniques for the maximum number of cases. The architecture of the algorithm explores the search space more efficiently and locates the thresholding values accurately, and fitness function value is influenced by the architecture and complexity of the methods. The proposed Masi-WCA method has generated optimum value and the second best value with a very small margin for the fitness function as shown in Table 3. Comparison of PSNR and MSE values obtained by BAT, PSO, WDO, MBO, GOA, and WCA with Masi entropy is depicted in Table 5. Masi entropy-based method has reported best performance in comparison with Tsallis entropy, whereas WCA has found best among BAT, PSO, WDO, MBO, and GOA. Table 7 compares the similarity in features of the original image and segmented image from the results obtained by using BAT, PSO, WDO, MBO, GOA, and WCA with Masi entropy, respectively. Tables 8 and 9 compare the entropy and computational time (seconds) for the Tsallis entropy and Masi entropy coupled with optimization techniques. Figure 4 depicts the segmented results of each image at threshold level $L=3$, 5, 8, and 12 acquired for Masi-BAT, Masi-PSO, Masi-WDO, Masi-MBO, Masi-GOA, and Masi-WCA. The main limitation of the proposed Masi-WCA method is that it takes more processing time for segmentation as compared to Masi-MBO methods, but Masi entropy coupled with different optimization techniques (Masi-BAT, Masi-PSO, Masi-WDO, Masi-MBO, Masi-GOA, and Masi-WCA) is always faster than Tsallis entropy-based optimization techniques (Tsallis-BAT, Tsallis-PSO, Tsallis-WDO, Tsallis-MBO, Tsallis-GOA, and Tsallis-WCA) which is reported in Table 9. However, Masi-WCA computes the best
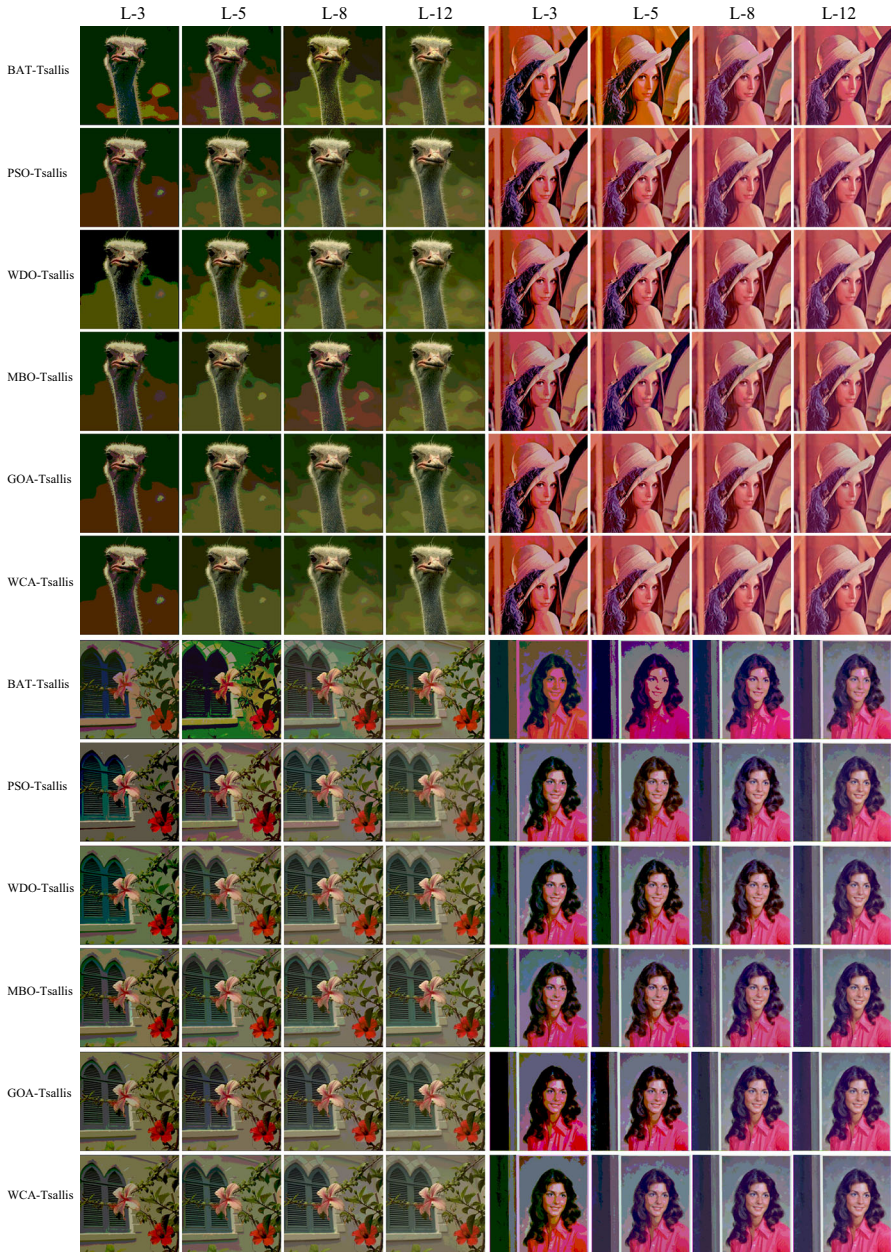
Fig. 3 Results showing 3-level, 5-level, 8-level, and 12-level segmented images using Tsalli-based multilevel thresholding approaches

quality of segmented images over Masi-MBO. In some cases, the proposed Masi-WCA method is not produced best or optimal values, but it has maintained the second best value of those cases. The entropy value of the segmented image of the proposed
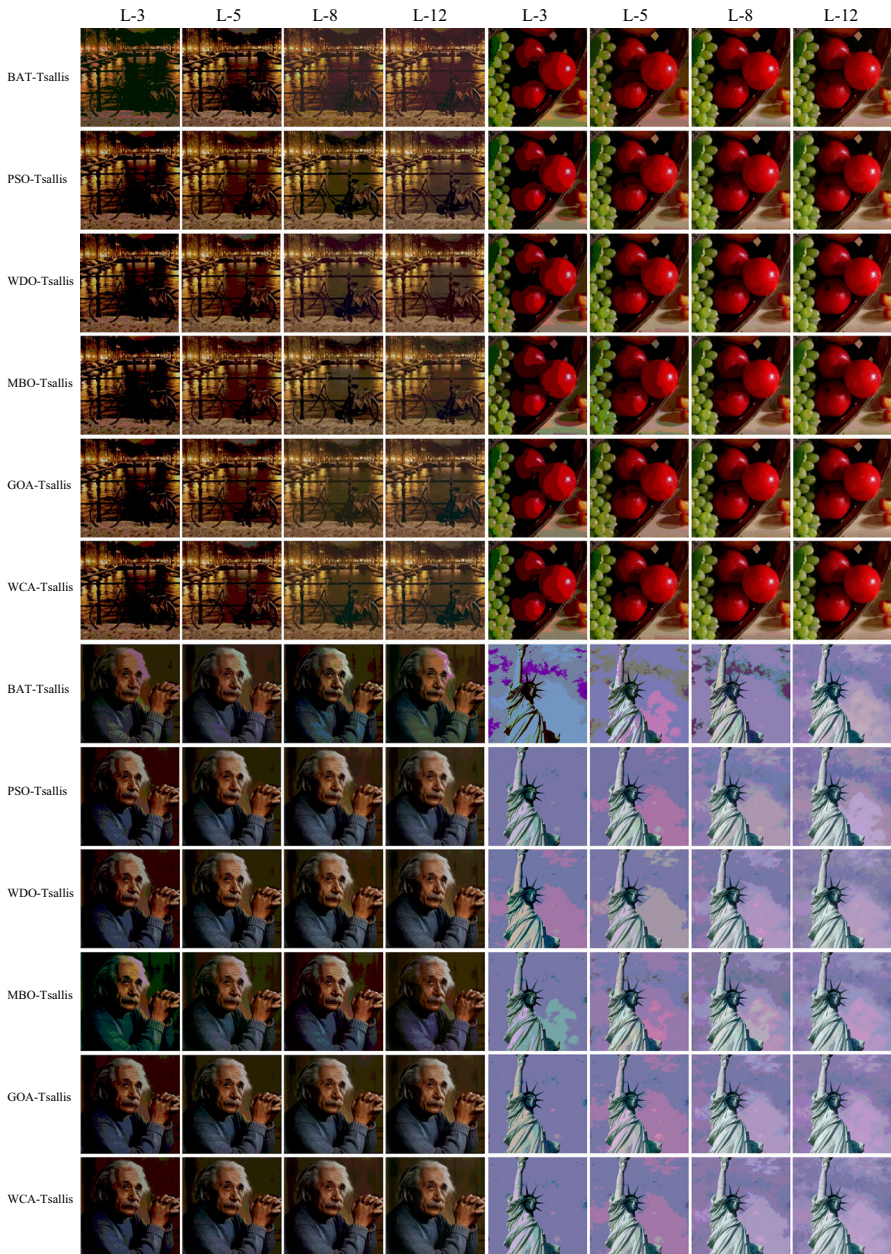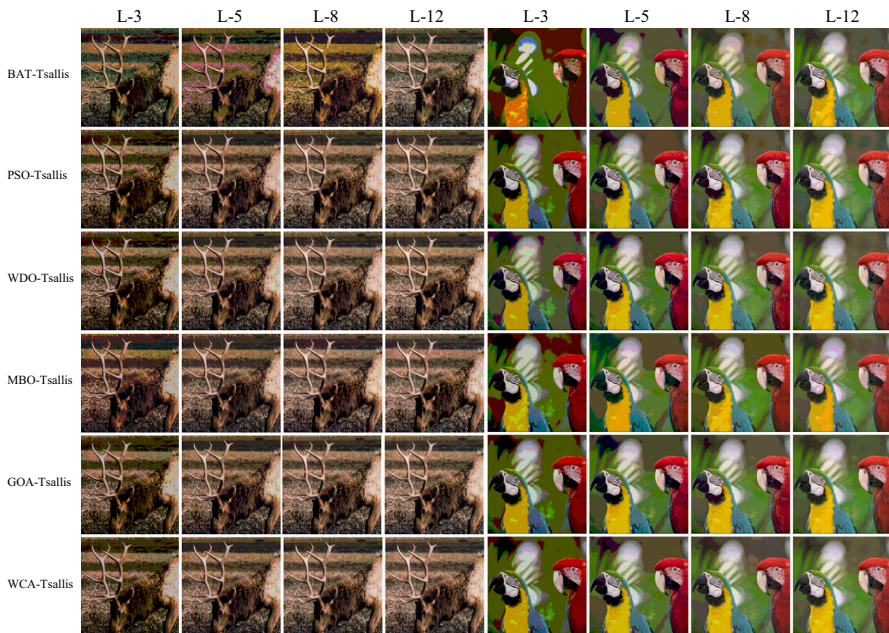
Fig. 3 continued

Masi-WCA method is a maximum value for 5-level, 8-level, and 12-level thresholding, whereas it holds the best and the second best value for 2-level thresholding for almost all cases.

Fig. 3 continued

Figures 11, 12, 13, 14, 15, and 16 depict the plots of the ME, MSE, PSNR, SSIM, FSIM and entropy of 8-level MT using Masi entropy, respectively, from which it can confirm that the performance of the proposed Masi-WCA approach is superior among BAT, PSO, WDO, MBO, GOA when coupled with Masi entropy. Figures 3 and 4 show the segmented results of each test image at 3-level, 5-level, 8-level, and 12-level of thresholding from which it can be visually investigated that proposed Masi-WCA method surpasses the Tsallis-WCA-based results. From Tables 2, 3, 4, 5, 6, 7, 8, and 9, it can be clearly identified that Masi entropy overcomes the Tsallis entropy-based methods and the statistical analysis of the proposed algorithm outclasses with respect to all methods.

4.4 Comparison of WCA-Masi with Other Algorithms

The accuracy of the proposed Masi-WCA multilevel thresholding algorithm is the highest among all other compared algorithms in terms of image segmentation process. Moreover, compared methods are not very effective to perform the optimal thresholds. The Masi-MBO method is an average method where the accuracy is a major concern, but Masi-GOA method is the second best approach for the multilevel thresholding of the color image segmentation. WCA, MBO, and GOA are the recently introduced optimization techniques which are not exploited for the image segmentation purpose.

However, Tsallis entropy is a very efficient algorithm but has slightly lower performance than Masi entropy (objective function). Since the objective function holds
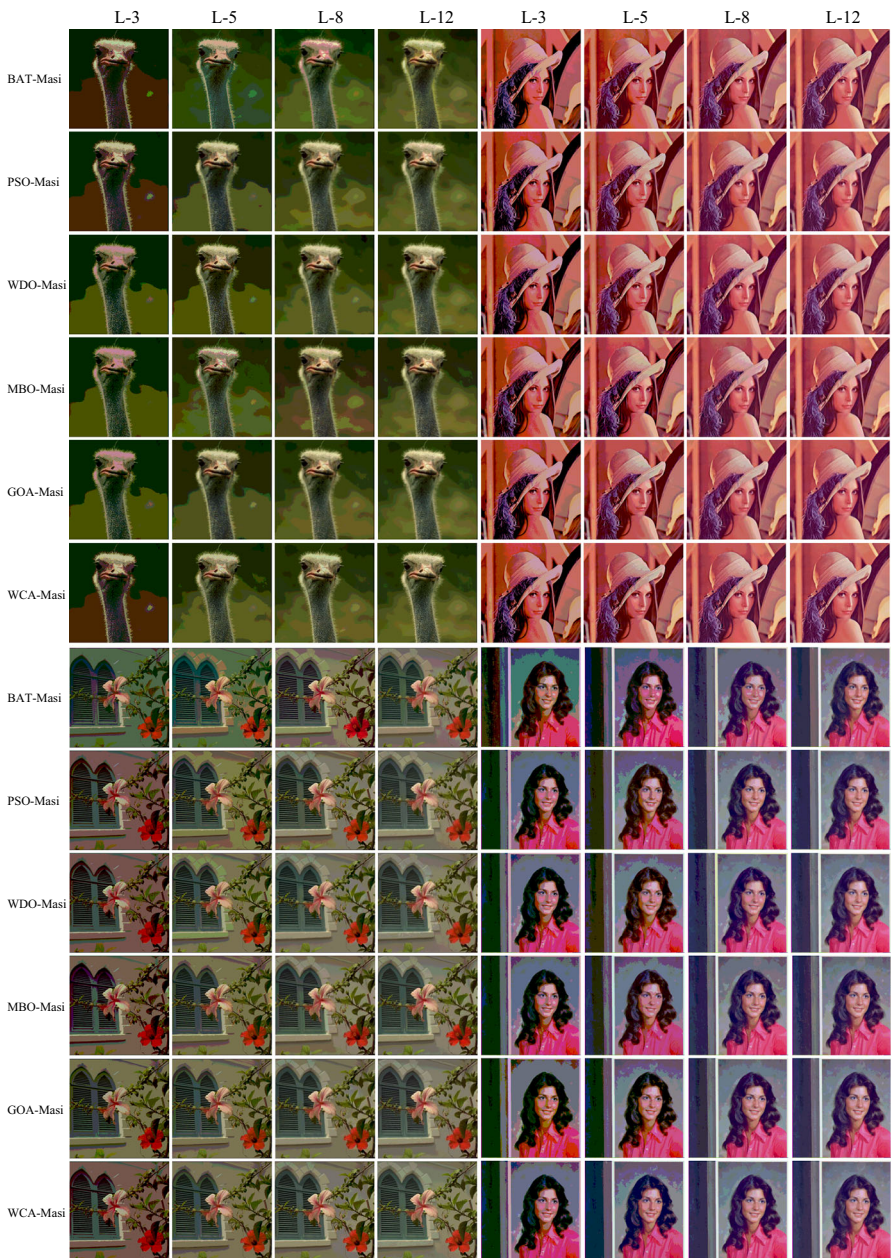
Fig. 4 Results showing 3-level, 5-level, 8-level, and 12-level segmented images using Masi-based multilevel thresholding approaches

the major importance in determining the threshold values, the mathematical model of Masi entropy is able to provide better thresholded results because of the non-extensive or additive information properties. WDO has fairly better results than PSO and BAT.
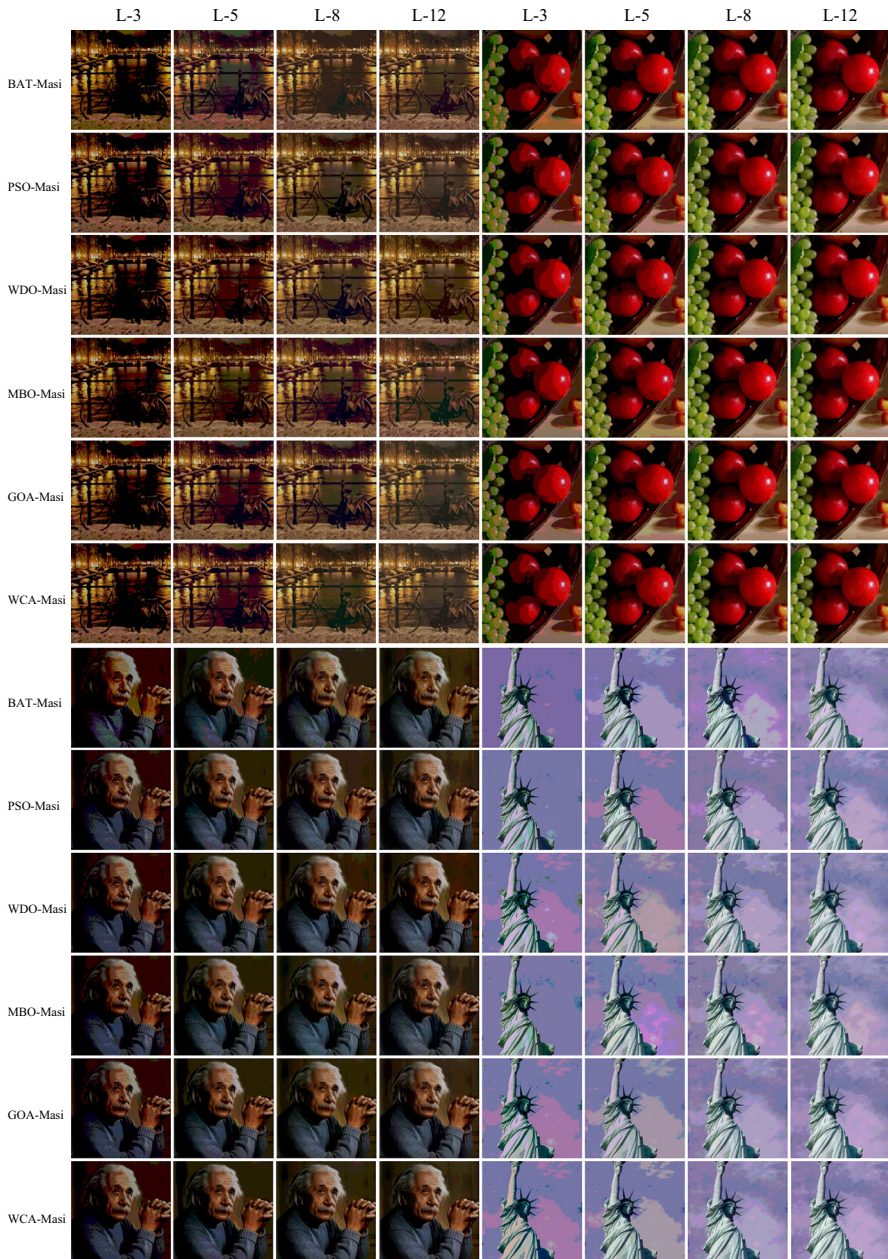
Fig. 4 continued

This is due to the poor capability of these algorithms in searching the accurate thresholding levels to separate the image pixels into homogenous regions. BAT has generated poorly segmented outputs at the lower and higher thresholding levels; GOA produces better outputs but not as better than WCA. In few cases, the GOA gives similar results
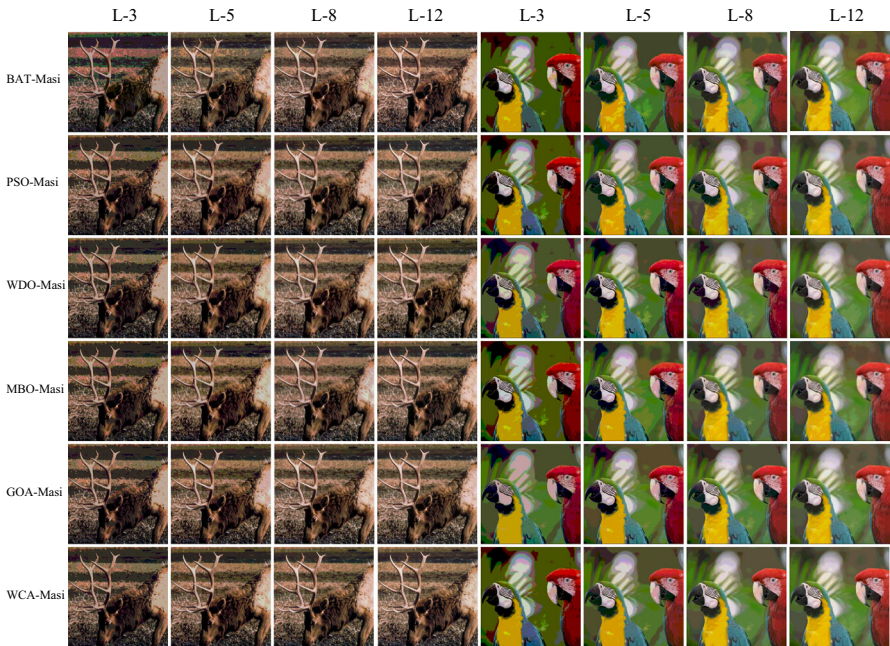
Fig. 4 continued

Fig. 5 Plots of 8-level ME using Tsallis
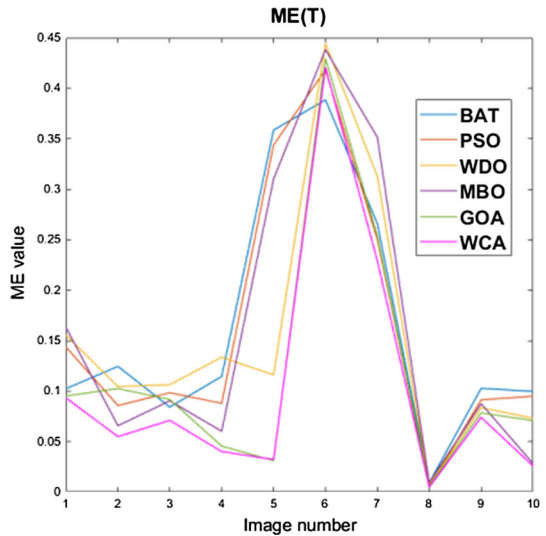
as the WCA. In some cases, WDO, PSO, and MBO optimization techniques have achieved better segmentation. But, the BAT and MBO are not very efficient in determining the threshold values accurately. The results of Masi-GOA have followed the performance of Masi-WCA, and Masi-GOA approach is fair at classifying pixels at high thresholding levels.

Fig. 6 Plots of 8-level MSE
using Tsallis
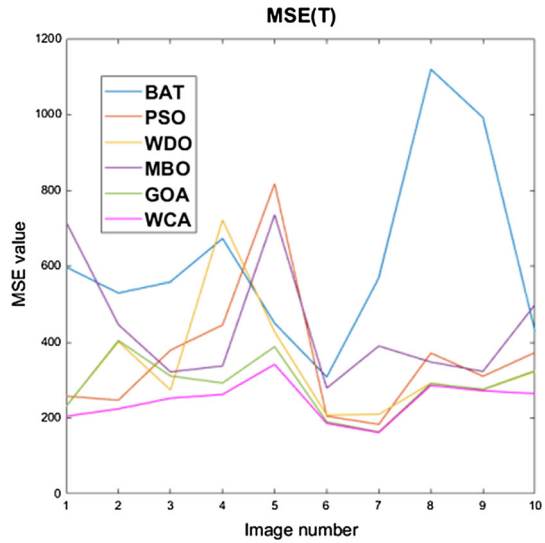
**Fig. 7** Plots of 8-level PSNR
using Tsallis
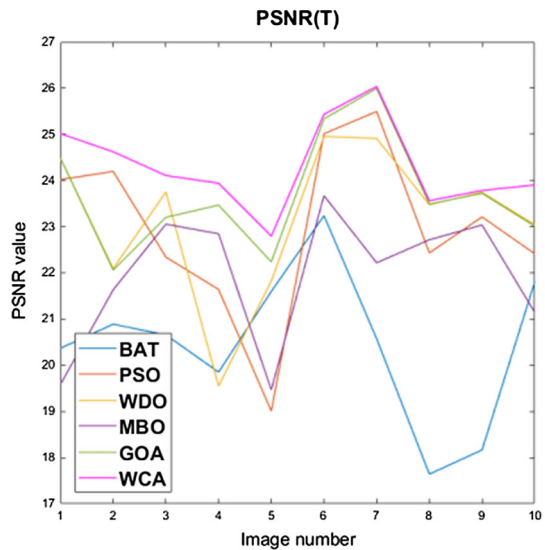
The results presented in this paper by proposed algorithm are superior in almost all the cases followed by some of the other recently developed metaheuristics algorithm. This action occurs because each image contains diverse features that characterize a particular optimization problem. Besides, the randomness of metaheuristic algorithms (ECA) produces some fluctuations in the results. For instance, if a threshold value is chosen through the metaheuristic that is not suitable, the segmented image probably will be not the best. Such condition merely can be identified by PSNR, MSE, SSIM, FSIM, and entropy because the objective function (Tsallis and Masi entropies) only offer information about how the intensities values are distributed in different regions.

Fig. 8 Plots of 8-level SSIM using Tsallis
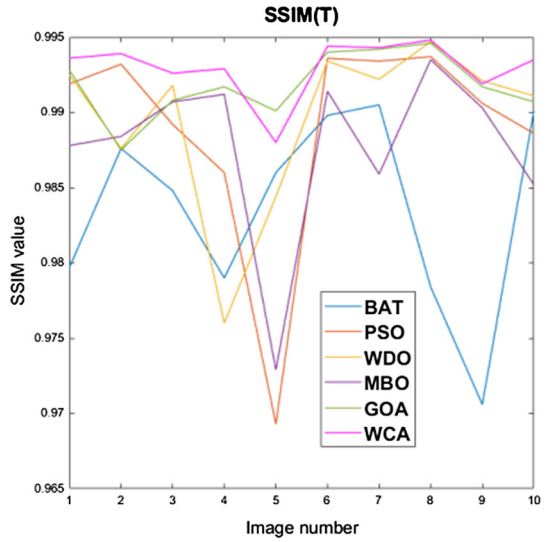
**Fig. 9** Plots of 8-level FSIM using Tsallis
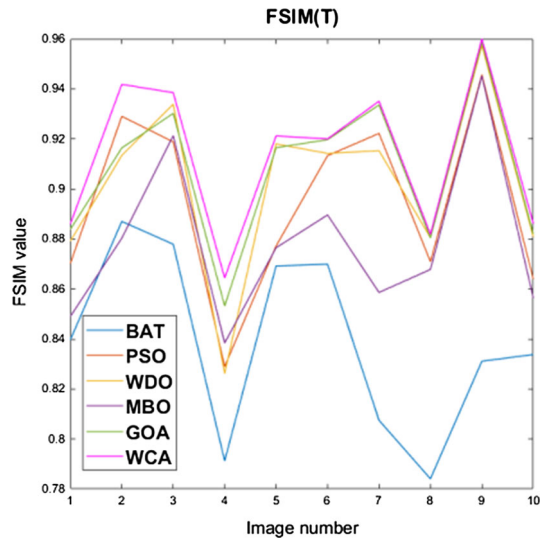
The analysis of convergence rate of IMG1 and IMG7 images using BAT, PSO, WDO, MBO, GOA, and WCA based on Tsallis and Masi entropies is shown in Figs. 17, 18, 19, and 20 for each R-G-B color channel individually. It is concluded that WCA convergence is faster as compared to other algorithms with respect to maximum objective values.

One of the advantages of the proposed Masi-WCA method is that the function values are reduced to near-optimum point in the early iterations. This may be due to the searching criteria and constraint handling approach of WCA where it initially searches a wide region of problem domain and rapidly focuses on the optimum solution. In general, the WCA offers competitive solutions compared with other metaheuristic

**Fig. 10** Plots of 8-level entropy using Tsallis
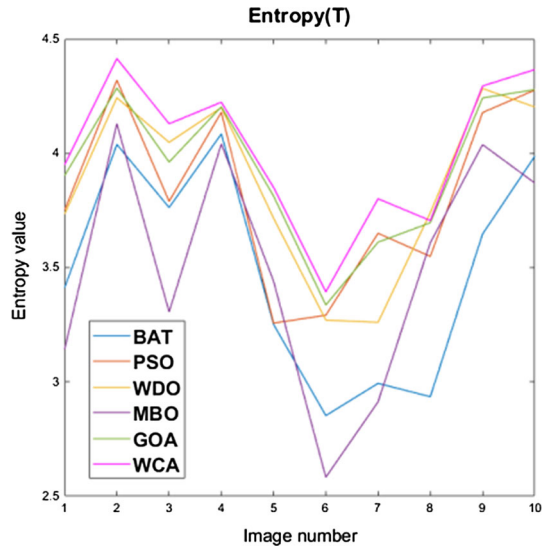

Fig. 11 Plots of 8-level ME using Masi
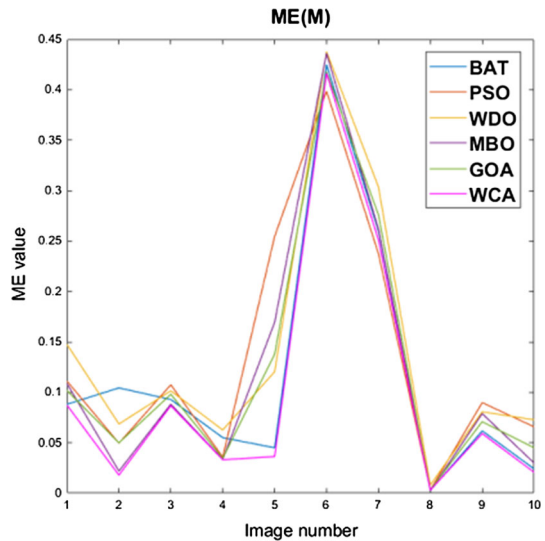
optimizers. However, the computational efficiency and quality of solutions given by the WCA depend on the nature and complexity of the underlined problem. This applies to the efficiency and performance of numerous metaheuristic methods. The WCA is used for solving the real-world optimization problems, in terms of the optimum solution; it provides better or close to the best value compared with BAT, PSO, WDO, MBO, and GOA. In terms of the convergence function evaluations, the WCA reached the best solution faster than other algorithms. Therefore, the use of WCA in multilevel thresholding adds more accuracy and flexibility in determining the optimal threshold values that can vibrantly distinguish different objects present in the image and produces

Fig. 12 Plots of 8-level MSE using Masi
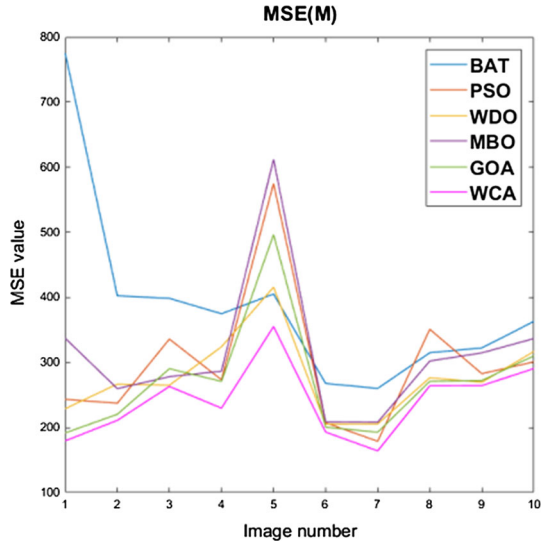
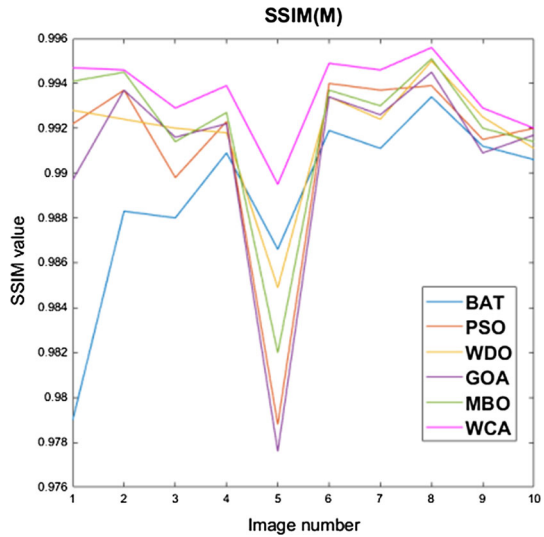**Fig. 13** Plots of 8-level PSNR using Masi
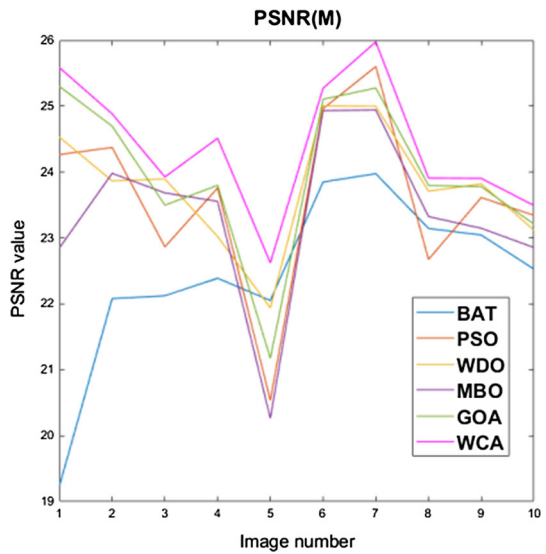
high-quality segmented color images. The proposed algorithm effectively deals with the uncertainties in color images with high randomness and multiple small targets with full of inherent uncertainty.
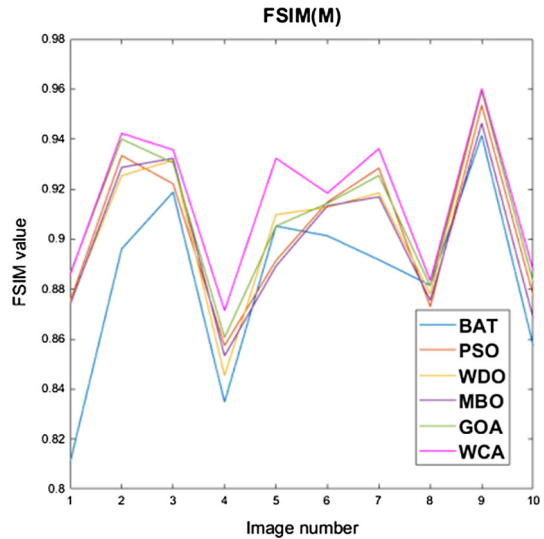
5 Conclusion

In this paper, a new color image multilevel thresholding method based on water cycle algorithm is proposed for segmentation. In this work, recently proposed optimization

Fig. 14 Plots of 8-level SSIM using Masi

Fig. 15 Plots of 8-level FSIM using Masi

algorithms such as BAT, PSO, WDO, MBO, GOA, and WCA have been employed to maximize Tsallis and Masi entropies to solve the problem of image segmentation by determining the optimum multilevel threshold values. From the results, it can be concluded that the proposed Masi-WCA method can be efficiently and effectively be used in color image thresholding operation. The qualitative and quantitative illustrations for almost all test images exhibit that the WCA outperforms the BAT, PSO, WDO, MBO, and GOA. The study also reports about the performance of the two entropy-based objective functions with each optimization technique, which confirms the superiority of the Masi over Tsallis entropy. In order to measure the performance of the proposed approach, entropy, MSE, ME, SSIM, FSIM, and PSNR have been utilized to

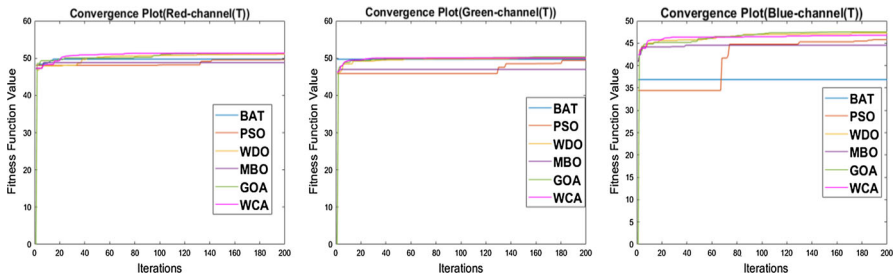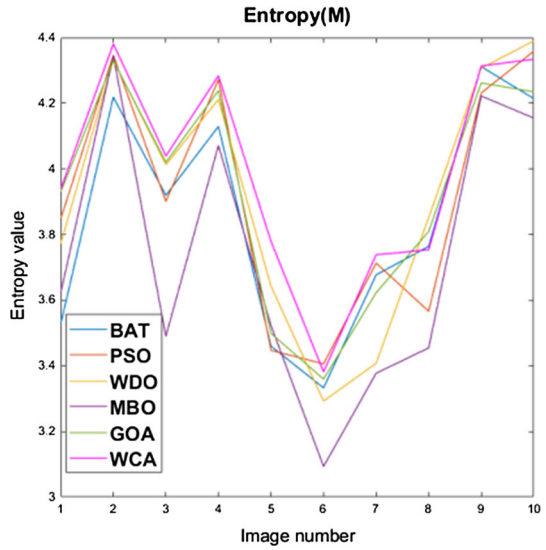**Fig. 16** Plots of 8-level entropy using Masi

Fig. 17 Convergence plots of 12-level MT using Tsallis entropy for each R-G-B channel of the color IMG1
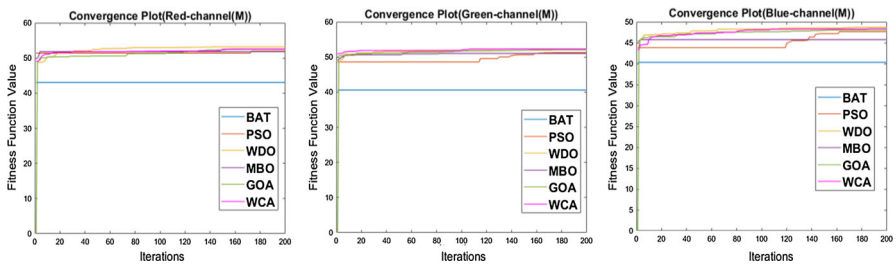

Fig. 18 Convergence plots of 12-level MT using Masi entropy for each R-G-B channel of the color IMG1

assess the quality of segmentation by considering the coincidences among the original images and respective segmented images. Even if individual entropies are considered, WCA outperforms all other optimization techniques considered in this paper. Hence, WCA has been proven to be superior to the rest of algorithms and also the Masi-WCA beats Tsallis-WCA in terms of efficiency and robustness. The experimental outcomes are encouraging and motivate futuristic research areas to apply WCA to other image
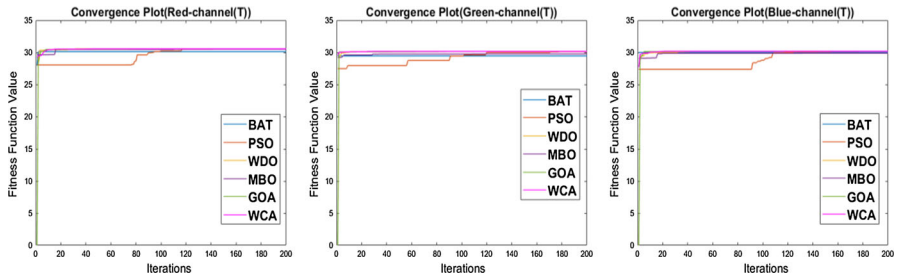
Fig. 19 Convergence plots of 5-level MT using Tsallis entropy for each R-G-B channel of the color IMG7
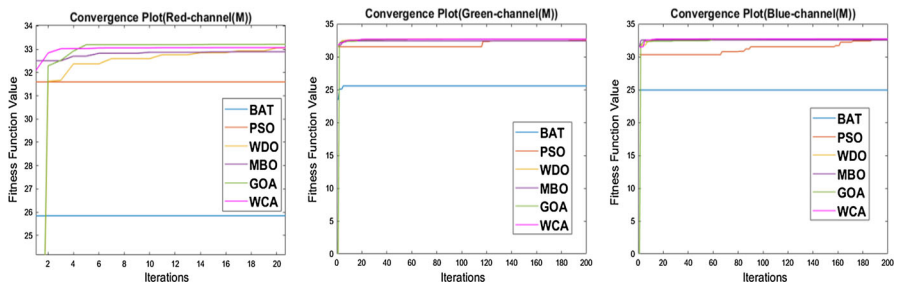
Fig. 20 Convergence plots of 5-level MT using Masi entropy for each R-G-B channel of the color IMG7

processing applications such as image enhancement, image denoising, image classification, and various computer-related problems. Furthermore, the performance of other traditional entropies can be estimated using WCA concept for multilevel color image segmentation.

References

1. A.K. Bhandari, A. Kumar, G.K. Singh, SVD based poor contrast improvement of blurred multispectral remote sensing satellite images, in *Computer and Communication Technology (ICCCT), 2012 Third International Conference on,* (IEEE, 2012), pp. 156–159
2. A.K. Bhandari, A novel beta differential evolution algorithm-based fast multilevel thresholding for color image segmentation. Neural Comput. Appl. (2018). https://doi.org/10.1007/s00521-018-3771-z
3. A.K. Bhandari, S. Maurya, A.K. Meena, Social spider optimization based optimally weighted otsu thresholding for image enhancement. IEEE J. Sel. Top. Appl. Earth Obs. Remote Sens. (2018). https://doi.org/10.1109/JSTARS.2018.2870157
4. Z. Bayraktar, M. Komurcu, J.A. Bossard, D.H. Werner, The wind driven optimization technique and its application in electromagnetics. IEEE Trans. Antennas Propag. **61**(5), 2745–2757 (2013)
5. A.K. Bhandari, A. Kumar, G.K. Singh, Feature extraction using normalized difference vegetation index (NDVI): a case study of Jabalpur city. Procedia Technol. **6**, 612–621 (2012)
6. A.K. Bhandari, V.K. Singh, A. Kumar, G.K. Singh, Cuckoo search algorithm and wind driven optimization based study of satellite image segmentation for multilevel thresholding using Kapur's entropy. Expert Syst. Appl. **41**(7), 3538–3560 (2014)
7. A.K. Bhandari, V. Soni, A. Kumar, G.K. Singh, Artificial Bee Colony-based satellite image contrast and brightness enhancement technique using DWT-SVD. Int. J. Remote Sens. **35**(5), 1601–1624 (2014)
8. A.K. Bhandari, V. Soni, A. Kumar, G.K. Singh, Cuckoo search algorithm based satellite image contrast and brightness enhancement using DWT–SVD. ISA Trans. **53**(4), 1286–1296 (2014)

9. A.K. Bhandari, A. Kumar, G.K. Singh, Improved knee transfer function and gamma correction based method for contrast and brightness enhancement of satellite image. AEU Int. J. Electron. Commun. **69**(2), 579–589 (2015)

10. A.K. Bhandari, A. Kumar, G.K. Singh, Modified artificial bee colony based computationally efficient multilevel thresholding for satellite image segmentation using Kapur's, Otsu and Tsallis functions. Expert Syst. Appl. **42**(3), 1573–1601 (2015)

11. A.K. Bhandari, A. Kumar, G.K. Singh, Tsallis entropy based multilevel thresholding for colored satellite image segmentation using evolutionary algorithms. Expert Syst. Appl. **42**(22), 8707–8730 (2015)

12. A.K. Bhandari, D. Kumar, A. Kumar, G.K. Singh, Optimal sub-band adaptive thresholding based edge preserved satellite image denoising using adaptive differential evolution algorithm. Neurocomputing **174**, 698–721 (2016)

13. A.K. Bhandari, A. Kumar, S. Chaudhary, G.K. Singh, A novel color image multilevel thresholding based segmentation using nature inspired optimization algorithms. Expert Syst. Appl. **63**, 112–133 (2016)

14. A.K. Bhandari, A. Kumar, G.K. Singh, V. Soni, Performance study of evolutionary algorithm for different wavelet filters for satellite image denoising using sub-band adaptive threshold. J. Exp. Theor. Artif. Intell. **28**(1–2), 71–95 (2016)

15. A.K. Bhandari, A. Kumar, S. Chaudhary, G.K. Singh, A new beta differential evolution algorithm for edge preserved colored satellite image enhancement. Multidimens. Syst. Signal Process. **28**(2), 495–527 (2017)

16. A.K. Bhandari, A. Kumar, G.K. Singh, V. Soni, Dark satellite image enhancement using knee transfer function and gamma correction based on DWT–SVD. Multidimens. Syst. Signal Process. **27**(2), 453–476 (2016)

17. P. Civicioglu, Backtracking search optimization algorithm for numerical optimization problems. Appl. Math. Comput. **219**(15), 8121–8144 (2013)

18. H. Eskandar, A. Sadollah, A. Bahreininejad, M. Hamdi, Water cycle algorithm–a novel metaheuristic optimization method for solving constrained engineering optimization problems. Comput. Struct. **110**, 151–166 (2012)

19. L. He, S. Huang, Modified firefly algorithm based multilevel thresholding for color image segmentation. Neurocomputing **240**, 152–174 (2017)

20. A.B. Ishak, Choosing parameters for Rényi and Tsallis entropies within a two-dimensional multilevel image segmentation framework. Phys. A **466**, 521–536 (2017)

21. J. Kittler, J. Illingworth, Minimum error thresholding. Pattern Recogn. **19**(1), 41–47 (1986)

22. A. Kumar, A.K. Bhandari, P. Padhy, Improved normalised difference vegetation index method based on discrete cosine transform and singular value decomposition for satellite image processing. IET Signal Proc. **6**(7), 617–625 (2012)

23. C.H. Li, C.K. Lee, Minimum cross entropy thresholding. Pattern Recogn. **26**(4), 617–625 (1993)

24. X. Li, J. Wang, A steganographic method based upon JPEG and particle swarm optimization algorithm. Inf. Sci. **177**(15), 3099–3109 (2007)

25. Y. Li, X. Bai, L. Jiao, Y. Xue, Partitioned-cooperative quantum-behaved particle swarm optimization based on multilevel thresholding applied to medical image segmentation. Appl. Soft Comput. **56**, 345–356 (2017)

26. Y.W. Lim, S.U. Lee, On the color image segmentation algorithm based on the thresholding and the fuzzy c-means techniques. Pattern Recogn. **23**(9), 935–952 (1990)

27. M. Masi, A step beyond Tsallis and Rényi entropies. Phys. Lett. A **338**(3–5), 217–224 (2005)

28. S. Mishra, M. Panda, Bat algorithm for multilevel colour image segmentation using entropy-based thresholding. Arab. J. Sci. Eng. **43**, 7285–7314 (2018)

29. F. Nie, P. Zhang, J. Li, D. Ding, A novel generalized entropy and its application in image thresholding. Signal Process. **134**, 23–34 (2017)

30. D. Oliva, E. Cuevas, G. Pajares, D. Zaldivar, V. Osuna, A multilevel thresholding algorithm using electromagnetism optimization. Neurocomputing **139**, 357–381 (2014)

31. S. Pare, A.K. Bhandari, A. Kumar, G.K. Singh, An optimal color image multilevel thresholding technique using grey-level co-occurrence matrix. Expert Syst. Appl. **87**, 335–362 (2017)

32. S. Pare, A.K. Bhandari, A. Kumar, V. Bajaj, Backtracking search algorithm for color image multilevel thresholding. SIViP **12**(2), 385–392 (2018)

33. S. Pare, A.K. Bhandari, A. Kumar, G.K. Singh, A new technique for multilevel color image thresholding based on modified fuzzy entropy and Lévy flight firefly algorithm. Comput. Electr. Eng. **70**, 476–495 (2018)
34. T. Pun, A new method for grey-level picture thresholding using the entropy of the histogram. Signal Process. **2**(3), 223–237 (1980)
35. A.K. Bhandari, A. Kumar, G.K. Singh. Improved feature extraction scheme for satellite images using NDVI and NDWI technique based on DWT and SVD. Arab. J. Geosci. **8**(9), 6949–6966 (2015)
36. S. Pare, A.K. Bhandari, A. Kumar, G.K. Singh, Rényi's entropy and Bat algorithm based color image multilevel thresholding, in *Machine Intelligence and Signal Analysis*, ed. by M. Tanveer, R. Pachori (Springer, Singapore 2019), pp. 71–84
37. A. K. Bhandari, M. Gadde, A. Kumar, G. K. Singh, Comparative analysis of different wavelet filters for low contrast and brightness enhancement of multispectral remote sensing images. in *2012 International Conference on Machine Vision and Image Processing (MVIP)*, Taipei (2012), pp. 81–86
38. S. Pare, A.K. Bhandari, A. Kumar, G.K. Singh, S. Khare, Satellite image segmentation based on different objective functions using genetic algorithm: a comparative study, in *Digital Signal Processing (DSP), 2015 IEEE International Conference on*. (IEEE 2015), pp. 730–734
39. P.K. Sahoo, G. Arora, Image thresholding using two-dimensional Tsallis–Havrda–Charvát entropy. Pattern Recogn. Lett. **27**(6), 520–528 (2006)
40. P. Sahoo, C. Wilkins, J. Yeager, Threshold selection using Renyi's entropy. Pattern Recogn. **30**(1), 71–84 (1997)
41. S. Saremi, S. Mirjalili, A. Lewis, Grasshopper optimisation algorithm: theory and application. Adv. Eng. Softw. **105**, 30–47 (2017)
42. M. Sezgin, B. Sankur, Survey over image thresholding techniques and quantitative performance evaluation. J. Electron. Imaging **13**(1), 146–166 (2004)
43. V. Soni, A.K. Bhandari, A. Kumar, G.K. Singh, Improved sub-band adaptive thresholding function for denoising of satellite image based on evolutionary algorithms. IET Signal Proc. **7**(8), 720–730 (2013)
44. W.H. Tsai, Moment-preserving thresolding: a new approach. Comput. Vis. Graph. Image Process. **29**(3), 377–393 (1985)
45. Z. Wang, A.C. Bovik, H.R. Sheikh, E.P. Simoncelli, Image quality assessment: from error visibility to structural similarity. IEEE Trans. Image Process. **13**(4), 600–612 (2004)
46. G.-G. Wang, S. Deb, Z. Cui, Monarch butterfly optimization. Neural Comput. Appl. (2015). https://doi.org/10.1007/s00521-015-1923-y
47. X.S. Yang, A new metaheuristic bat-inspired algorithm, in *Nature Inspired Cooperative Strategies for Optimization (NICSO 2010)*. (Springer, Berlin, Heidelberg, 2010), pp. 65–74
48. L. Zhang, L. Zhang, X. Mou, D. Zhang, FSIM: a feature similarity index for image quality assessment. IEEE Trans. Image Process. **20**(8), 2378–2386 (2011)

Affiliations

Pankaj Kandhway[1] · Ashish Kumar Bhandari[1]

Pankaj Kandhway
pankaj.kandhway@gmail.com

[1] Department of Electronics and Communication Engineering, National Institute of Technology Patna, Patna 800005, India